# Cascades of sub-decadal, channel-floodplain changes in low-gradient, non-vegetated reaches near a dryland river terminus:

Li, Jiaguang; Tooth, Stephen; Yao, Guangqing

*Published in:*
Earth Surface Processes and Landforms

*DOI:*
10.1002/esp.4512

*Publication date:*
2019

# Cascades of sub-decadal, channel-floodplain changes in low-gradient, non-vegetated reaches near a dryland river terminus: Salar de Uyuni, Bolivia

Jiaguang Li,[1,2*] Stephen Tooth[3], Guangqing Yao[1]

[1] Key Laboratory of Tectonics and Petroleum Resources (China University of Geosciences), Ministry of Education, Wuhan 430074, China. (jiaguangli@cug.edu.cn, jiaguangli@gmail.com)

[2] State Key Laboratory of Oil and Gas Reservoir Geology and Exploration (Chengdu University of Technology), Chengdu 610059, China

[3] Department of Geography and Earth Sciences, Aberystwyth University, Aberystwyth, SY23 3DB, UK

## Abstract

The terminus of the ephemeral Río Colorado is located at the margins of Salar de Uyuni, Bolivia, the world's largest salt lake. The low-gradient (<0.0006 m $m^{-1}$), non-vegetated reaches approaching the terminus provide an excellent natural laboratory for investigating cascades of channel-floodplain changes that occur in response to quasi-regular flows (at least once annually) and fine-grained sediment supply (dominantly silt and clay). High-resolution satellite imagery (<0.65 m, various dates from 2004 onwards) and field data reveal widespread, pronounced and rapid morphodynamics on sub-decadal timescales, including channel erosion and chute cutoff formation, and development of crevasse channels and splays, floodouts (unchannelled surfaces at channel termini), and erosion cells (floodplain scour-transport-fill features). In particular, following high annual precipitation (>400 mm) in 2004-2005 and two subsequent high magnitude daily precipitation events (~40 mm), all of which led to widespread flooding, numerous crevasse splays formed between 2004 and 2016, avulsions occurred at nearby floodouts, and erosion cells downstream of the splays and floodouts underwent striking morphological changes. High-precision GPS data reveal two preferential localities for erosion cell development: partially or fully abandoned channels with crevasse splay remnants, and topographic lows between channels. In this overall low-gradient setting, comparatively high gradients (up to ~0.0006 m $m^{-1}$) at the edge of splay deposits and topography created by crevasses and abandoned channels may initiate knickpoint retreat and thereafter erosion cell development. Abandoned channels with splays tend to give rise to narrow, deep erosion cells, while topographic lows promote relatively shallow, wide erosion cells. In both situations, erosion cells may extend upslope and downslope, and eventually connect to form straight channels. The channel-floodplain morphodynamics near the Río Colorado terminus extend previous analyses of low-gradient, dryland river systems, particularly because the lack of vegetation and quasi-regular floods drive cascades of rapid changes on sub-decadal timescales.

Keywords: crevasse splay; dryland river terminus; floodout; floodplain; knickpoint; erosion cells

## 1. Introduction

Knowledge of contemporary patterns and rates of channel-floodplain geomorphological processes is important for anticipating and managing changes that may result from climate or land-use change but also can play a crucial role in reconstructing Quaternary fluvial palaeoenvironments and deciphering older fluvial sedimentary rock records (Miall, 1996; Davidson et al., 2011; Tooth et al., 2013). While the majority of research has focused on the channels and floodplains associated with perennial rivers in humid regions (e.g. Bridge, 2003), in recent decades increasing attention has been directed towards channel-floodplain morphodynamics in the lower reaches of ephemeral or intermittent dryland rivers, including those systems that terminate on unchannelled alluvial plains, in aeolian dunefields, in seasonal wetlands, or at the margins of periodically inundated pans and playas (Tooth, 2000a, 2013). A varied and somewhat confusing terminology has arisen to describe the lower reaches and termini of such dryland rivers, including terminal fan (e.g. Mukerji, 1976; Kelly and Olsen, 1993), floodout zone and floodout (e.g. Tooth, 1999a, b, 2004; Tooth et al., 2002, 2014), and terminal splay and terminal splay complex (e.g. Lang et al., 2004; Fisher et al., 2008). The newer, broader term distributive fluvial system (DFS) – used to describe a river that emerges from valley confinement into a sedimentary basin to form a radial network of channels and deposits (Davidson et al., 2013) – subsumes many of these terms and related others such as megafan, alluvial fan and fluvial fan. Regardless of the term applied, the channel-floodplain morphodynamics in dryland settings influence the resulting stratigraphy and sedimentary architecture, with many systems being characterised by narrow channel sand and gravel bodies inset within, or encased by, more extensive fine-grained overbank deposits, and by a general downvalley decrease in the ratio of channel to overbank deposits (e.g. Tooth, 1999b). Such knowledge is vital for improving interpretation and economic exploration of some ancient fluvial systems, some of which may form potentially significant hydrocarbon reservoirs (e.g., Miall, 1996; Mjøs et al., 1993; Bridge, 2003; van Toorenenburg et al., 2016).

The varied terms used to describe the lower reaches and termini of dryland rivers are commonly associated with a variety of descriptive and genetic terms for specific channel and floodplain features. These terms have arisen from the study of modern-day fluvial systems in various climatic and physiographic settings, including low-gradient drylands. For instance, crevasse channels and splays have been described from floodout zones in central Australia, with many having erosional bases that are incised up to ~2 m into pre-splay, fine-grained overbank sediments (Tooth, 2005; Millard et al., 2017). Some terminal splay complexes in central Australia are characterised by an amalgamation of the deposits of numerous individual splays that diverge from the characteristic distributary channel network (e.g. Lang et al., 2004). Floodplain channels have been defined as channels forming only through overbank flooding processes and extending to the floodplain margin or being far away from the trunk channel (Mertes et al., 1996; Stølum, 1998, Fagan and Nanson, 2004; Trigg et al., 2012). David et al. (2017) further developed the term to refer to any channel segment operating on the floodplain independently from the trunk channel.

These definitions of floodplain channels could be extended to include a feature of some low-gradient dryland river systems, namely the erosion cell or scour-transport-fill (S-T-F) sequence (Pickup, 1985, 1991). Erosion cells transfer water and sediment from upslope erosional networks to downslope depositional complexes. First described from dryland river floodplains in central Australia (Pickup, 1985, 1991; Bourke and Pickup, 1999), partially or fully analogous features have since been described from other dryland Australian floodplains (Wakelin-King and Webb, 2007) and seasonal wetlands in dryland South Africa (Tooth et al., 2014). Erosion cells are active during overbank flow and may have long-term effects both on the morphodynamics and sedimentology of low-gradient dryland fluvial systems (e.g. Pickup, 1991; Bourke and Pickup, 1999; Wakelin-King and Webb, 2007; Tooth et al., 2014). For instance, shifting mosaics of erosion cells not only shape the immediate landsurface but may also influence longer-term channel-floodplain development and widely and deeply rework sediment, with a potentially significant impact on fluvial stratigraphy and sedimentary architecture.

Although increasingly recognised and described in outline, high-resolution data to characterise the spatial and temporal morphodynamics of these various dryland channel and floodplain features remain limited. Most previous studies have been conducted in dryland settings with at least partial vegetation cover (e.g. trees, shrubs and grasses), and the vegetation has been shown to play a variety of roles, such as strengthening channel banks, displacing channel flow onto adjacent floodplains, and either locally increasing floodplain surface erosional resistance or focusing scour and incision (e.g. Bourke and Pickup, 1999; Tooth, 2000b, 2005; Wakelin-King and Webb, 2007; Fisher et al., 2008; Tooth et al., 2014). Such studies provide valuable insights into the importance of biogeomorphological interactions but for comprehensive treatment of the full spectrum of dryland fluvial conditions, attention also needs to be directed to the more poorly vegetated or non-vegetated settings that are characteristic of some dryland rivers in hyperarid, arid or semiarid settings. This is particularly important for improving interpretations of ancient, pre-vegetation (i.e. pre-Silurian) fluvial systems where complexes of channel and floodplain features (e.g. splays, floodplain channels) developed in the absence of any above- or below-ground vegetative influences (Gibling and Davies, 2012).

As a case in point, Ielpi et al.'s (2018) review of pre-vegetation floodplains included extensive reference to modern non-vegetated fluvial systems, with examples drawn both from humid exorheic systems (Icelandic coastal plains) and dryland endorheic systems (Death Valley in California, USA and Salar de Uyuni, Bolivia). Salar de Uyuni is the world's largest salt lake, and is periodically supplied with water and sediment by low-gradient, ephemeral rivers such as the Río Colorado. This river has been the focus of extensive previous studies that have shown, *inter alia*, how high-resolution satellite imagery can be useful for quantifying channel-floodplain morphology and dynamics in this poorly or non-vegetated dryland setting, including meander bend dynamics, the development of crevasse splays, and avulsions (Donselaar et al., 2013; Torres Carranza, 2013; Li, 2014, 2018; Li et al., 2014a, b, 2015a, b, 2018; Li and Bristow, 2015; Sandén, 2016). Erosion cells have been noted in the upstream parts of the Río Colorado catchment (Li et al., 2015b) and are also prominent features farther downvalley but have not been investigated in any detail. Ielpi et al.'s (2018) review made reference to much of this previous work, highlighting how the Río Colorado provides a modern analogue for pre-vegetation floodplains that were variably composed of features such as floodbasins, splay complexes, and minor levees. Significantly, however, Ielpi et al. (2018) did not mention erosion cells, probably owing to the fact that there are insufficient detailed studies of these features from the Río Colorado or other dryland fluvial settings to enable the development of criteria that would aid their recognition in ancient fluvial successions.

In this paper, we complement and extend these previous studies by investigating in greater detail than previously the interlinked channel-floodplain morphodynamics that took place along the Río Colorado from 2004 to 2016, including erosion cell development. We combine high resolution (<0.65 m) satellite imagery with new field data and focus on the channel-floodplain morphodynamics in the low-gradient, non-vegetated reaches approaching the river terminus at the margins of the Salar de Uyuni. The study has three aims: 1) to characterise the patterns, timing and rates of change of a range of channel and floodplain features; 2) to interpret and explain the key controls and processes of change, focusing especially on erosion cells and their relation to wider cascades of channel-floodplain changes; and 3) to compare the morphodynamics in these low gradient, non-vegetated reaches with the morphodynamics of other terminal dryland systems.

## 2. Study area

The study area lies within the catchment of Salar de Uyuni, Bolivia (Fig. 1A and 1B), a salt flat with an area of ~10 000 km$^2$ and an elevation of ~3650 m above sea level. The lake and its catchment are located in the southern part of the Altiplano basin, which formed as part of the Andean oceanic-continental convergent margin. Eastward subduction of the oceanic Nazca Plate beneath the continental South American Plate (Dewey and Bird, 1970; Horton and DeCelles, 2001) has led to development of the central Andes during the Cenozoic, with regional horizontal shortening leading to increasing thickness of the continental crust (Isacks, 1988; Jordan et al., 1997) and regional uplift and volcanism forming elevated regions such as the Altiplano. Drainage in the Altiplano basin is endorheic (Fig. 1B) and the basin is filled with Tertiary to Quaternary fluvial and lacustrine sediments and volcaniclastic deposits (Horton et al., 2001; Elger et al., 2005). The basin has an overall semiarid climate, with an annual precipitation of more than 800 mm in the north and less than 200 mm in the south (Argollo and Mourguiart, 2000) and an annual evapotranspiration potential of 1500 mm (Grosjean, 1994; Risacher and Fritz, 2009). The north-south decrease in precipitation is due to the prevailing low pressure weather systems, whereby strong low-level northwesterly winds with warm, moist, and unstable air flow along the eastern flank of the central Andes and give rise to convection precipitation. Poleward low-level airflow helps to maintain the intense convection (Lenters and Cook, 1999).

The Río Colorado terminus is located at the southeastern margin of the Salar de Uyuni (Fig. 1) and its 15 000 $km^2$ catchment comprises upper Ordivician to Tertiary clastic sedimentary and igneous rocks, with Quaternary sediments widespread (Marshall et al., 1992; Horton et al., 2001). Despite some prominent fault escarpments in the catchment (Bills et al., 1994; Baucom and Rigsby, 1999; Rigsby et al., 2005; Donselaar et al., 2013), the study area has been tectonically quiescent in the late Pleistocene and Holocene. Although highly variable, mean annual rainfall in the study area is ~185 mm and the 24 hour maximum daily precipitation only rarely exceeds 40 mm (Li, 2014; Li and Bristow, 2015) (Fig. 2). Annual precipitation is greatly exceeded by the mean annual potential evapotranspiration of 1500 mm, resulting in a local aridity index (annual precipitation divided by annual potential evaporation) of 0.12 (United Nations Environment Program, 1992). As such, the meandering Río Colorado is ephemeral with river flow occurring mainly in response to thunderstorms in the austral summer (December through March - Li et al., 2014a). Although there are no flow gauging records, small to moderate (sub-bankfull) river flow events occur one or more times in most years, with larger events (bankfull or above) occurring at least once every few years. According to local accounts, following heavy rainfall and significant flow in the Río Colorado and other local rivers, water depths in Salar de Uyuni can reach up to 10 m deep, but analysis of Landsat time-series satellite imagery (1985-2011) indicates that the lake typically dries out in the intervening winter months (Li et al., 2014b). Field data on sediment loads are limited, but grain-size analyses indicate that the lower Río Colorado system is dominated by silt and clay with subordinate very fine sand.

Previous studies of the lower Río Colorado have revealed the overall low gradient, with a maximum gradient of 0.000575 m $m^{-1}$ declining to ~0.000148 m $m^{-1}$ near the river terminus (Li et al., 2015b). The river is characterised by a complex of active, partially active and abandoned channels, but one dominant meandering trunk channel is evident (Donselaar et al., 2013). Along this trunk channel, there is a prominent downstream reduction in width, depth and cross-sectional area (Li et al., 2014a). Vegetation index analysis indicates that the Río Colorado river terminus is essentially non-vegetated, likely due to the characteristically dry and saline environment (Fig. 1D; see also Li and Bristow, 2015, their Figs. 1C and 11).

## 3. Data and methods

High-resolution satellite imagery (QuickBird-2, WorldView-2, Pléiades) with spatial resolutions of <0.65 m enables visualization of the spatial and temporal development of channel-floodplain morphology. To examine sub-decadal scale changes, five sets of images of the study area (2004/2005, 2007, 2010/2011, 2013, 2016) were analysed (Table 1). Due to greater data availability and quality, two sets of images (2004/2005, 2013) have been used for analysing the entire lower 30 km of the river approaching the terminus. Newer images were registered to the reference image of 2004/2005 using the remote sensing image analysis software ENVI. The RMS error was calculated from the difference between the actual and predicted coordinates when the warp image was registered to the reference image, and was less than 1.5 pixels. Along with field measurements, these satellite images were used for quantifying a range of channel-floodplain parameters, including bankfull channel width. Measurements of these parameters were made for each kilometre reach starting from the Río Colorado bridge (Fig. 1C, see red dot in lower right). In this ungauged river, the width measurements provided a robust basis for calculating bankfull discharge using Bjerklie's (2007) model, as has been done successfully for lengthy reaches of other dryland rivers (e.g. Larkin et al., 2017).

To complement previous investigations of channel gradient in the reaches approaching the river terminus (Li et al., 2015b), in this study we focused on documenting channel-floodplain topography and floodplain gradient in greater detail. During field campaigns in November 2012 and 2015, high-precision data were retrieved by a Trimble R7 dual frequency geodetic global positioning system (GPS) device (see Li et al. (2015b) for details on processing of similar datasets). Using these GPS data, topographic models of erosion cells were constructed using interpolation, and down-valley and cross-valley floodplain gradients were plotted and quantified. Along with the satellite-based width measurements and the discharge calculations, these GPS-derived gradients were used to calculate specific (unit) stream powers for the Río Colorado and various other channel-floodplain features by using van den Berg's (1995) approach.

## 4. Results

Previous work has shown that the lower Río Colorado trunk channel undergoes a downstream reduction in channel width, depth and cross-sectional area before the river terminates at the margins of Salar de Uyuni (Donselaar et al., 2013). These downstream channel geometry changes result in an increasing proportion of flood flows being diverted overbank. Combined with the fine-grained sediments and the lack of vegetation, the quasi-regular flood pulsing promotes widespread, pronounced and rapid changes in channel-floodplain morphology. Our new analyses, undertaken using more recent high-resolution satellite imagery, provide additional insights into these characteristic changes on sub-decadal timescales, examples of which are described below.

## 4.1 Channel and floodplain morphological changes

### *4.1.1 Development of chute cutoffs, crevasse splays and avulsions*

Chute cutoffs have occurred on different floodplain channels of the Río Colorado, as illustrated in Figures 3 and 4. For the more northerly cutoff – located ~16 km downstream from the Río Colorado bridge (Fig. 1C, see red dot in lower right) – satellite imagery shows no evidence of chute or crevasse channels in late 2004 (Fig. 3A) but by late 2007 at least two poorly-defined channels had formed across the neck between the upstream and downstream parts of a meander bend (Fig. 3B). These two channels had rationalised to one distinct chute channel by mid 2013 (Fig. 3C). Further incision and widening of the chute channel occurred between 2013 and 2016, resulting in completion of the cutoff and partial abandonment and infilling of the former meander bend (Fig. 3D). In addition, along the partially abandoned bend, bank breaching led to formation of a distinct crevasse channel between 2013 and 2016 (Fig. 3D). This crevasse conveyed water to the floodplain during peak flow, promoting the formation of erosion cells through floodplain scour (Fig. 3D; see also Section 4.1.2).

Other floodplain channels have experienced significant erosion that also has been accompanied by chute cutoff and crevasse channel and splay formation. For example, along a 3.12 km long floodplain channel that diverges from the left bank of the trunk channel ~7 km downstream from the Río Colorado bridge (Fig. 4), satellite imagery shows that the channel experienced migration with a total erosional area of 29 357 $m^2$, with concomitant formation of chute cutoffs and crevasse splays. Along this channel, more than 40 new crevasse channels and splays formed from late 2004 to late 2007, many of which expanded in subsequent years (Fig. 5). Widening and deepening of one of these crevasse channels (NCS2) ultimately may form a local avulsion, with increasing amounts of flow and sediment now being diverted from the left bank of the main floodplain channel (Fig. 5D).

This floodplain channel terminates at a floodout located to the west of the Río Colorado trunk channel (Figs 1C and 6). In late 2004, the main channel leading to the floodout curved northward with several crevasse channels diverting westward (Fig. 6A). Subsequent enlargement of several of these crevasse channels resulted in avulsion, with increasing flow and sediment redistribution to the west (Fig. 6B-C). These changes to the complex of channels and crevasse splays meant that by early 2016 two new main channels followed more westerly pathways to the floodout, with the original, northward-directed, main channel now more subordinate (Fig. 6D).

*4.1.2 Development of erosion cells*

Erosion cells previously have been noted in the upstream reaches of the Río Colorado catchment (Li et al., 2015b) but new satellite and field data collected as part of this study show that in the study area, most erosion cells tend to be located on the medial and distal parts of the lower Río Colorado floodplain.  These data reveal two preferential locations for erosion cell development: partially or fully abandoned floodplain channels with crevasse splay remnants (Figs. 7 and 8), and floodplain topographic lows between channels (Fig. 9).  The abandoned floodplain channels tend to be broadly parallel to the flow direction in the active trunk channel but commonly are perpendicular to the flow direction in crevasse channels that diverge from the trunk channel.  Along these abandoned floodplain channels, some of the numerous crevasse splay remnants develop into erosional cells (Fig. 7).  Satellite imagery shows that those crevasse splay remnants with the same orientation as the crevasse channels emanating from the trunk channel (i.e. southeast to northwest in Figs. 7 and 8) have a higher probability of erosion cell development.

Along the abandoned floodplain channels, the length of erosion cells is typically between 100 m and 400 m, with widths averaging ~8 m and depths locally >50 cm along the transport sections (Table 2).  Potentially, however, the length of erosion cells could be up to 1 km in situations where two different cells become connected.  By contrast, erosion cells that have developed in floodplain topographic lows tend to be longer and wider.  These erosion cells can reach up to few kilometers in length, with widths typically many tens of meters but depths remaining mostly <10 cm in the transport sections (Fig. 9).  These erosion cells are supplied by overbank flow, by flow emanating from crevasse splays developed along the channels adjacent to the topographic low, or by flow that continues beyond the end of channel termini onto floodouts (Fig. 9).

**4.2 Channel geometry and hydraulics**

Figure 10 illustrates changes in the geometry and hydraulics of the lower Río Colorado trunk channel between 2004 and 2013.  For both years, mean channel width displays an overall downstream decrease.  With the exception of 16-18 km downstream where there is a small local width increase, the upstream reaches (distance 0-16 km) show an exponential width decrease while more downstream reaches (distance 18-30 km) show a more linear width decrease (Fig. 10A).  The data reveal a slight overall increase in width between 2004 and 2013 (Figs. 10A and B).

Channel geometry changes are closely related to changes in channel hydraulics. Using Bjerklie's (2007) model, estimated bankfull discharge also shows a slight overall increase between 2004 and 2013 (Fig. 10C). Specific stream power also shows a slight overall increase between 2004 and 2013, with the most prominent increase occurring between 4 and 13 km downstream (Fig. 10D). Calculations at other channel-floodplain locations (Table 2) show that specific stream powers remain low overall, but tend to be highest (~5.36 W $m^{-2}$) in the erosion cells (Table 2).

### 4.3 Floodplain gradient

High-precision GPS data reveal the details of channel and floodplain topography, and enable quantification of down-valley and cross-valley gradients. Previous studies of the lower Río Colorado have revealed that a maximum gradient of 0.000575 m $m^{-1}$ declines to ~0.000148 m $m^{-1}$ near the river terminus (Li et al., 2015b). The new GPS data collected as part of this study confirm these overall low gradients but provide significant additional details. The data show that the gradient of the floodplain channel near the cut-off occurrence (Fig. 3) is ~0.00037 m $m^{-1}$ while the down-valley gradient adjacent to the crevasse channels (Fig. 4) and the abandoned floodplain channel with erosion cells (Fig. 6) are ~0.00023 m $m^{-1}$ and ~0.00022 m $m^{-1}$, respectively. The data also show that the cross-valley gradient at the edge of the crevasse splays located upstream of the erosion cells shown in Figure 8 is relatively high (0.00059 m $m^{-1}$) compared to the crevasse splays themselves (0.00018 m $m^{-1}$, Fig. 11A). GPS mapping of the topography of an erosion cell located in the downstream part of a floodout (Figs. 11B and C) shows the typical characteristics of incision in the upper (scour) and middle (transport) sections but shallowing both in the downstream (fill) sections and laterally away from the cell.

## 5. Interpretation

The combination of satellite imagery and field investigations of the lower Río Colorado reveals widespread, pronounced, and rapid channel and floodplain changes on a sub-decadal timescale. Many changes appear to be linked, with meander bend cutoffs, crevasse channels and splays, avulsions, and erosion cells developing in close proximity. In these low gradient, non-vegetated dryland river reaches, interrelated issues thus include establishing: 1) the precipitation and flow controls on the channel-floodplain morphodynamics; and 2) the underlying processes driving the identified dynamics.

### 5.1 Precipitation and flow controls

There are no flow gauging records for the lower Río Colorado, but precipitation data from 1975 through 2017 for the study area indicate strong variations (Fig. 2). For the period 1975-2006, an annual precipitation total >380 mm has occurred four times, whereas after 2006 annual precipitation total never exceeded 232 mm and in most years was <200 mm.  High annual precipitation totals tend to be indicative of multiple (possibly consecutive) days of lower magnitude precipitation events (Li and Bristow, 2015) and lead to an increased number of river flow events.  Conversely, for the period 1975 through 2011, only one maximum daily precipitation event greater than 40 mm has occurred but from 2012 onwards, three daily maximum precipitation events of ~40 mm have occurred (2012-2013, 2014-2015, 2016-2017), two of which are within the timeframe considered in this study (2004-2016).  According to analyses undertaken in a parallel study (Li et al., 2018), such high daily precipitation values result from approximately 40-year events, and are associated with extreme floods, characterized in this system by extensive overbank flooding.

In a previous study that used precipitation data and intermediate resolution Landsat imagery time series from 1975 through 2001, Li et al. (2014a) argued for clear links between precipitation events, discharge, and channel and floodplain changes.  That precipitation, flooding and morphodynamic changes are linked is not surprising, as has been shown by many other studies of dryland river response to individual flood events (see Tooth, 2013), including in the study area (Li et al., 2018).  Rarely, however, has there been detailed study of the impacts of two or more closely-spaced floods on dryland river morphology (Milan et al., 2018) but the rainfall record, availability of high-resolution satellite imagery, and rapidity of change on the lower Río Colorado provides an unusual opportunity to do so.

For the study period 2004-2016, the high annual precipitation total in 2004-2005 and the two high magnitude daily precipitation events in 2012-2013 and 2014-2015 all resulted in widespread flooding.  These events likely account for the observed widespread, pronounced and rapid changes in the lower Río Colorado, including the overall widening of the trunk channel (Fig. 10A) and other channel-floodplain morphodynamic changes (Figs 3-7).

For instance, chute channel formation occurred between 2004 and 2007 (Fig. 3) and the initiation process can be attributed mainly to the low magnitude but consecutive precipitation events that resulted in the high annual precipitation totals in 2004-2005 (418 mm) and 2005-2006 (306 mm). The image of 2013 (Fig. 3C) indicates that chute channel cutoff was complete by this time, perhaps as a response to the high daily maximum precipitation event in 2012-2013 that likely resulted in widespread overbank flooding.

Similarly, the widespread formation of crevasse splays between 2004 and 2007 (Figs. 4 and 5) seems to have corresponded with the high annual precipitation total during that period.  In addition, significant floodplain erosion occurred during two periods (2004-2007 and 2007-2013), indicating that both the high annual precipitation total and the maximum daily precipitation events could have contributed. The 2016 imagery (Figs 4D and 5D) indicates the enlargement of many floodplain channels and crevasse channels, which may have resulted from the high maximum daily precipitation event and associated flooding in 2014-2015.

Morphological changes at floodouts (Fig. 6) also most likely can be attributed to the coupled effects of high annual precipitation totals and high maximum daily precipitation events. The 2007 imagery (Fig. 6B) indicates a new flow path approaching the floodout as well as an abundance of new splay channels, perhaps reflecting the high annual precipitation total in 2004-2005. The 2013 and 2016 imagery (Figs 6C-D) indicates subsequent changes that probably occurred during the high maximum daily precipitation events in 2012-2013 and 2014-2015.

The development of erosion cells (Fig. 7) at the edge of crevasse splays appear to be related more to maximum daily precipitation events alone. For the period 2004-2010, only limited development of erosion cells occurred, despite the high annual precipitation total in 2004-2005 (Figs 7A-B). By contrast, the 2013 and 2016 imagery (Figs 7C-D) reveals prominent erosion cell development, probably reflecting the high maximum daily precipitation events in 2012-2013 and 2014-2015 that likely resulted in widespread overbank flooding. During such floods, development of new crevasse splays upslope (Fig. 8) would have supplied overbank flow to the upper parts of the erosion cells, with potential specific stream power reaching up to ~5.36 W $m^{-2}$ in the transport sections (Table 2).

## 5.2 Processes of channel-floodplain dynamics

Despite the slight tendency for channel widening between 2004 and 2013, an overall downstream decrease in channel width, depth and cross-sectional area is still evident (Figs 10A-B). This downstream decrease leads to an increasing proportion of flow being diverted overbank during peak floods (cf. Donselaar et al., 2013; Li and Bristow, 2015), with bank and levee breaching commonplace along the non-vegetated channel margins. This strong channel-floodplain connectivity has led to cascades of changes throughout the wider study reach, including along floodplain channels that essentially operate independently of the trunk channel. These cascades can be illustrated by considering the processes that contribute to the development of the following sets of features.

### *5.2.1 Chute cutoffs, splays and avulsions*

Chute cutoffs have occurred along partially abandoned floodplain channels (Fig. 3) and are a natural outcome of cutback erosion on non-vegetated bends combined with chute channel incision across the poorly-vegetated floodplain surfaces that lie between the upstream and downstream parts of the bends. Once cutoff is complete, waning flow and infilling of partially abandoned bends and longer reaches of abandoned floodplain channels leads to reduction in channel cross-sectional areas and even greater overbank displacement of flood flows.  Widespread, rapid breaching of non-vegetated banks has led to significant erosion and lateral migration of some floodplain channels, which may lower levees and further promote overbank flow (Li and Bristow, 2015), resulting in initiation and enlargement of numerous crevasse channels and associated splays between 2004 and 2016 (Fig. 4).  As shown by Li et al.'s (2014a) and Li and Bristow's (2015) analyses for the earlier part of this timeframe, in some locations, new or enlarged splays coalesce or overlap.  For instance, where a new crevasse develops in the space between two existing splays, compensational stacking of splay sediment occurs, ultimately leading to infilling of the topographic lows adjacent to the trunk channel and maintenance of the overall low down-valley and cross-valley gradients (Li et al., 2014a; Li and Bristow, 2015).  In other locations, crevasse channels widen and deepen, drawing increasing amounts of flow from the trunk channel (e.g. Fig. 5D).  As shown by Donselaar et al. (2013), such crevasse channel enlargement ultimately can lead to avulsion, with the trunk channel being gradually abandoned in favour of the new channel.  Between 2004 and 2016, such changes in flow pathways have been most clearly demonstrated near channel termini at floodouts (Fig. 6).

### *5.2.2 Abandoned channels, splays, topographic lows and erosion cells*

Erosional cells are prominent features of the study area (e.g. Figs 7, 9, 12).  The processes of initiation and subsequent development of erosion cells depend on whether they form in association with partially or fully abandoned channels with crevasse splay remnants (Fig. 7), or in floodplain topographic lows (Fig. 9).

Along abandoned channels, satellite imagery indicates that crevasse splay remnants that have roughly the same orientations as active crevasse channels along the trunk channel are favoured for erosion cell development (Figs 7 and 8).  During peak discharge events, general overbank flooding may occur but much flow is directed from the trunk channel through the active crevasse channels and splays and toward the remnant crevasse splays farther downslope.  High-precision GPS data reveal locally high relief at the edge of the active crevasse splays, which increases flow energy and erosion potential (Fig. 11A).  In addition, the crevasse splay remnants provide preferential flow pathways, concentrating overbank flow from upslope and/or dispersing flow downslope away from the abandoned channel on the rising limb of flood hydrographs, but may also serve as conduits for return flow from the floodplain to the abandoned channel on the falling limb (cf. Donselaar et al., 2013; Li and Bristow, 2015).  In some instances, the elevation drop between the floodplain surface with its remnant splays and the bed of the abandoned channel can initiate knickpoints.  Satellite imagery shows clearly how some crevasse splay remnants have rapidly developed since 2004, with headward-retreating channels (scour sections of erosion cells) having incised floodplain sediments on the upslope side of the abandoned channel (Figs 7B-C), deeper channels (transport sections) having formed perpendicular to the original flow direction along the abandoned channel (Figs 7C-D), and shallower distributary channel networks (fill sections) having developed on the downslope side (Figs 7C-D). Over time, the headward-retreating channels extend upstream toward the currently active splays, which themselves may be subject to erosion on their steepened downslope margins.

In floodplain topographic lows, flow is derived from overbank flow or from flow that spreads beyond channel termini across floodouts. Due to the low gradients and stream powers, only limited incision occurs in these unconfined flows. When these flows intersect a channel or a crevasse channel with orientations that are perpendicular, however, the elevation drop between the floodplain or floodout surface and the channel base can also initiate knickpoints in the form of headward-retreating channels. These headward-retreating channels (source) may rationalise into single channels farther downslope (transfer), before dispersing as networks of small distributaries (fill) (Fig. 9). Alternatively, the unconfined flow spreading across floodouts can be directed into the headward-retreating channel networks of pre-existing erosion cells located downslope. On the low gradient floodouts, headward-retreat rates and incision depths in these erosion cells are limited, but when avulsions near to channel termini lead to major distribution of flow (e.g. Fig. 6), new headward-retreating channel networks can form downslope.

Over longer timeframes (decades to centuries), erosion cells may develop in parallel and/or become linearly distributed between two partially or fully abandoned channels (Fig. 12). Individual erosion cells may extend upslope and downslope, increasing the potential for cell-to-cell connection. If connection occurs, this may lead to a relatively straight channel formed between two older abandoned channels. This straight channel may be characterised by its cross-cutting relationship with older generations of channels and crevasse channels (Fig. 13). We speculate that in an otherwise typically meandering river system (Li et al., 2015b), many relatively straight channel reaches may be derived from the connection of originally linearly distributed erosion cells.

## 6. Discussion

The low gradient, non-vegetated lower reaches of the Río Colorado provide an excellent natural laboratory for investigating channel-floodplain morphodynamics that occur on sub-decadal timescales in response to quasi-regular flood pulsing. Our new analyses of the changes taking place between 2004 and 2016 complement and extend knowledge of the changes that have taken place in previous decades, including crevasse splay formation and avulsion (e.g. Donselaar et al., 2013; Li et al., 2014a). Over timescales of centuries to millennia, these morphodynamics contribute to the creation of a complex fluvial topography that likely is associated with considerable subsurface stratigraphic complexity. Although knowledge of the deeper subsurface sedimentology in the study area is limited, comparisons and contrasts nonetheless can be made with the channel-floodplain morphodynamics and sediments of other terminal dryland river systems, including terminal fans, floodout zones and floodouts, and terminal splay complexes.

### 6.1. Longer term fluvial morphodynamics and stratigraphic development

During the Quaternary, the water level and volume in the Salar de Uyuni has fluctuated dramatically, with phases of lake expansion and contraction occurring in response to wetter and drier climate intervals, respectively (Donselaar et al., 2013). At present, and despite short-term fluctuations in water level, the relatively dry climate corresponds with an overall lake lowstand, and the lower reaches of the Río Colorado and other local rivers terminate on the former lake bed (termed the 'lower lacustrine coastal plain' by Donselaar et al. (2013)). Li et al. (2015) have documented the sediment dispersal processes through the Río Colorado system, revealing a clear linear downstream decrease in coarser bedload sediments (i.e. gravel, medium to coarse sand) and a corresponding increase in finer suspended load sediments (i.e. clay, silt, subordinate fine sand) in the lower reaches. In such a Lowstand Systems Tract, vertical accommodation increase is limited, and sediment accumulation is characterized mainly by progradation and lateral expansion of the fluvial system rather than by vertical accumulation (Donselaar et al., 2013). Consequently, channel-floodplain morphodynamics such as meander migration and cutoff, crevasse splay development and avulsion have formed a radiating system of abandoned and active channel and floodplain features. This has resulted in thin (<2 m) but laterally extensive networks of amalgamated channel fill, point bar and crevasse splay deposits that overlie older (pre-late Holocene) lacustrine sediments (Donselaar et al., 2013; Li et al., 2014a; Li and Bristow, 2015). Minor surface reworking occurs in response to short-lived periods of lake expansion, as well as from subsequent dessication cracking, salt crust development, and aeolian deflation (e.g. Li and Bristow, 2015), but the sheet-shaped stratigraphic architecture is preserved (Donselaar et al., 2013). An avenue for future work might be to characterise the surface and subsurface sediments of the lower Río Colorado in greater detail, with a view to exploring more explicitly its potential application as an analogue for thin-bedded hydrocarbon reservoirs (e.g. van Toorenenburg et al., 2016; Li, in press).

### 6.2 Comparison with other terminal dryland river systems

These insights into the longer term fluvial morphodynamics and stratigraphic development provide a basis for comparing and contrasting the lower Río Colorado with other terminal dryland river systems.

In their study of avulsion processes, Donselaar et al. (2013) considered whether the reaches approaching the Río Colorado terminus correspond to the model developed for terminal fans (e.g. Kelly and Olsen, 1993), which implies a system of simultaneously active, multiple (distributary) channels. They concluded that the network of cross-cutting channels in the lower reaches of the Río Colorado is not the product of coeval distributary channels, with just one single channel being dominant during low flow periods. Older, partially or fully abandoned channels may be inundated during higher flow periods and only remain visible on the surface because vertical accommodation increase is limited and they have not been buried by younger sediment. Donselaar et al. (2013) suggested that their findings supported a new fluvial model for the terminus of low-gradient, semi-arid fluvial systems, in which a single main channel may change its position by successive multiple random (as opposed to nodal) avulsions.

In their study of crevasse splay morphodynamics, Li and Bristow (2015) compared the reaches approaching the Río Colorado terminus with the floodout zones of the Sandover, Sandover-Bundey and Woodforde Rivers in central Australia (Tooth, 1999a, b, 2000b, 2005). Both the lower Río Colorado and the central Australian systems are characterised by overall downstream decreases in channel cross-sectional areas, development of crevasse splays, and avulsions but, as noted by Li and Bristow (2015), there are also differences. For instance, the very low gradient, silt- and clay-dominated, non-vegetated lower Río Colorado contrasts with the steeper (~0.0005-0.0015), gravelly sand-dominated, partially vegetated reaches of the central Australian channels, and its termination on an periodically-flooded, saline, playa margin is quite different to the unchannelled but non-saline, alluvial plains that mark the termini of the central Australian channels.

In previous investigations of the lower Río Colorado, the term ‘terminal splay’ has been used to describe discrete splay deposits at channel termini, partly to distinguish these deposits from crevasse splays developed along channel reaches (Donselaar et al., 2013; Li et al., 2014a; Li and Bristow, 2015). This is a more restricted use of the term than has been applied to some fluvial systems that terminate on the margins of playas in central Australia (Lang et al., 2004; Fisher et al., 2008). For instance, the lower Neales River on the western margins of Lake Eyre is characterised by numerous individual splays that diverge from a distributary channel network but the terms ‘terminal splay’ and ‘terminal splay complex’ have tended to be used to describe the system as a whole, not individual features (e.g. Lang et al., 2004; Fisher et al., 2008). The lower Río Colorado has some physiographic, morphological and sedimentological similarities with the lower Neales River and other nearby systems but also many differences; for instance, the very low gradient, silt- and clay-dominated, non-vegetated lower Río Colorado contrasts with the steeper (~0.002), sandier, partially vegetated Neales River system (Lang et al., 2004).

These comparisons and contrasts illustrate the difficulties of consistently applying terminology to large dryland river systems that have been subject to long histories characterised by spatially complex morphodynamic and sedimentological changes. Consequently, broader terms such as distributive fluvial system (DFS) that subsume many of these and other related terms (Hartley et al., 2010; Weissmann et al., 2010; Davidson et al., 2013) may be more useful for describing and classifying the lower Río Colorado and other similar rivers. The use of distributive – as opposed to distributary – does not imply a system of coeval, multiple channels, but simply that the system is composed of radial network of active, partially active and abandoned channels and associated deposits. Observations from a range of modern DFS in aggradational continental sedimentary basins suggest that in some instances the formative DFS channel does not retain the same dimensions downstream, with intrinsic thresholds leading to breakdown of the main channel into smaller channels, and possibly to disintegration and termination of channelised flow. Davidson et al. (2013) suggest that three or four zones in DFS can be distinguished by fluvial morphology and behaviour and associated floodplain characteristics, with Zones 3 and 4 being the most distal. Future work might focus on comparing the morphological and sedimentological characteristics of the lower Río Colorado with the characteristics of other single thread, sinuous (meandering) and anabranching DFS (Davidson et al., 2013) and seeing whether this comparison provides support for the suggested zonation.

### 6.3 Comparative patterns and rates of change

Regardless of issues surrounding the application of the most appropriate descriptor, along many of these low-gradient, low energy, terminal dryland rivers, local topographic and other environmental factors (e.g. soil properties) can be a key influence on patterns of water and sediment movement, leading to a multiplicity of landforms of diverse origin, substrate type and hydroperiod (cf. Tooth, 1999a). The development of erosion cells is a case in point; as shown by this study, subtle changes in local topographic relief can be very important in determining the locations of scour, transport and fill that define these fluvial landforms (Section 5.2.2). Along the lower Río Colorado, for instance, the absence of vegetation means that overbank flow hydraulics are particularly sensitive to local topographic relief, with the potential for scour and incision increasing wherever there are increases in local gradient, such as at the margins of crevasse splays and in depressions formed by abandoned channels and crevasse channels (e.g. Fig. 7).

The non-vegetated nature of the lower Río Colorado contrasts with other dryland river systems where erosion cells and analogous features have been described, including floodplains and floodouts in central and south-eastern Australia (Pickup, 1985, 1991; Bourke and Pickup, 1999; Wakelin-King and Webb, 2007) and seasonal wetlands in South Africa (Tooth et al., 2014). In these Australian and South African systems, local topography is an important influence but the role of vegetation in the formation and development of erosion cells and analogous features also has been emphasised strongly. For instance, floodouts (i.e. the fill zone of many erosion cells) commonly serve as seed banks, with associated vegetation growth (e.g. grasses, shrubs, trees) helping to initiate and maintain floodout development by increasing hydraulic roughness and trapping sediment. In addition, the binding action of roots on floodout sediments helps to prevent or slow headcutting channels that may form on locally steepened gradients at the distal margin of floodouts and so serve as the scour zone for the next erosion cell downvalley (Bourke and Pickup, 1999; Wakelin-King and Webb, 2007; Tooth et al., 2014). In the Blood River wetlands, for instance, despite regular (seasonal) floods, headcutting channels formed on the locally steepened (~0.001-0.014 m $m^{-1}$) distal margin of unchannelled reedbeds have only widened slightly and extended a few tens of metres upvalley over a 70–80 year period (Tooth et al., 2014). By contrast, along the non-vegetated lower Río Colorado, pronounced erosion and deposition has led to the rapid development of erosion cells on sub-decadal timescales, with rates of headcut retreat being several orders of magnitude faster (Fig. 7), and with the potential for connection of originally linearly distributed erosion cells to form straight channel reaches (Figs 12 and 13). Ongoing monitoring of the rapidly developing lower Río Colorado thus may provide additional unparalleled opportunities to document in greater detail the erosional and depositional dynamics involved in erosion cell development, and how these features link into wider cascades of flood-driven, channel-floodplain changes in poorly or non-vegetated dryland settings.

The Río Colorado is unusual but not unique, and similar dynamics may characterize the lower reaches of other dryland rivers, such as the Amargosa River in Death Valley, California, USA (e.g. Ielpi et al., 2018) and little known systems on the margins of salt lakes near the Huobusun Lake in northwestern China (Figure 14). In these locations, morphodynamic studies might be complemented by investigations of the impact of floodplain channel (including erosion cell) development on sediment reworking, and its potential impact on fluvial stratigraphy and sedimentary architecture. This would help develop a wider range of recognition criteria to aid with interpretation of channel-floodplain features in ancient (especially pre-vegetation) fluvial successions (e.g. Ielpi et al., 2018). Collectively, such studies might help to provide generic, more widely applicable insights into fluvial landscape and sedimentary dynamics in low-gradient, terminal dryland rivers.

## 7. Conclusions

The lower reaches of the Río Colorado near its terminus on the margins of Salar de Uyuni, Bolivia, has undergone widespread, pronounced and rapid channel-floodplain changes during the last two decades. A combination of satellite image analysis and field investigations reveals evidence for cascades of changes that have included channel erosion and chute cutoff formation, as well as the development of crevasse channels and splays, erosion cells and floodouts. In particular, numerous crevasse splays formed between 2004 and 2016, with many being linked with avulsions and the development of floodouts and erosion cells. High-precision GPS data reveal two preferential localities for erosion cell development: abandoned channels with crevasse remnants, and floodplain topographic lows between channels. The former localities tend to promote narrow but deep erosion cells while the latter tend to give rise to relatively long and wide erosion cells. High-precision GPS data show that the gradient (~0.00059 m $m^{-1}$) at the edge of crevasse splays where erosion cells are abundant is more than twice as high as the downvalley floodplain gradient approaching the Río Colorado terminus, and this relatively high gradient is a key factor promoting erosion cell development in an otherwise low gradient terminal dryland river system. Erosion cells distributed between channels may extend upstream and downstream and eventually connect, ultimately forming newer, straighter channels.

Study of the Río Colorado complements and extends previous investigations of low-gradient, terminal dryland rivers. The findings provide an additional point of comparison and contrast with other dryland rivers that have been variously termed terminal fans, floodout zones, terminal splays, and distributive fluvial systems (DFS). Further study of the lower Río Colorado may provide information appropriate for its inclusion in preliminary databases of global DFS (Hartley et al., 2010; Weissmann et al., 2010). In addition, the lower Río Colorado and similar dryland rivers provide valuable opportunities to gain insights into the rapid channel-floodplain dynamics that can occur where quasi-regular flood pulsing on fine-grained sediments is unaffected by vegetation. For erosion cells in particular, this provides unparalleled opportunities for monitoring in detail the erosional and depositional dynamics involved in their development, and thus for gaining more generic insights into how their development may link to wider cascades of flood-driven changes in low-gradient, terminal dryland river systems. Further morphological and sedimentological studies of such rivers will add to our knowledge of modern dryland fluvial sedimentary environments, with implications for improved reconstructions of Quaternary fluvial systems and interpretations of ancient fluvial sedimentary rock outcrop, especially in pre-vegetation systems (Ielpi et al., 2018).

## Acknowledgements

This research was supported by Open Fund (PLC20180502) of State Key Laboratory of Oil and Gas Reservoir Geology and Exploration (Chengdu University of Technology), the National Natural Science Foundation of China (No. 41602121), the Fundamental Research Funds for the Central Universities, China University of Geosciences (Wuhan) (No. CUG150616), and Open Fund (TPR-2017-01) of Key Laboratory (Ministry of Education) of Tectonics and Petroleum Resources (China University of Geosciences) and the Scientific Research Foundation for the Returned Overseas Chinese Scholars, State Education Ministry. JL thanks the Hubei Province Chenguang Program for Young Scientists for supporting an international scholar visit.

## References

Argollo J, Mourguiart P. 2000. Late Quaternary climate history of the Bolivian Altiplano. Quaternary International **72**: 37–51.

Baucom PC, Rigsby CA. 1999. Climate and lake-level history of the northern Altiplano, Bolivia, as recorded in Holocene sediments of the Rio Desaguadero. Journal of Sedimentary Research **69**: 597-611.

Bills BG, de Silva SL, Currey DR, Emenger RS, Lillquist KD, Donnellan A, Worden B. 1994. Hydro-isostatic deflection and tectonic tilting in the central Andes: initial results of a GPS survey of Lake Minchin shorelines. Geophysical Research Letters **21**: 293–296.

Bjerklie DM. 2007. Estimating the bankfull velocity and discharge for rivers using remotely sensed river morphology information. Journal of Hydrology **341**: 144–155.

Bourke MC, Pickup G. 1999. Fluvial form variability in arid central Australia. In Varieties of Fluvial Form, Miller AJ, Gupta A. (eds), Wiley, Chichester: 249–271.

Bridge JS. 2003. Rivers and Floodplains: Forms, Processes and the Sedimentary Record. Blackwell, Oxford.

David SR, Edmonds DA, Letsinger SL. 2017. Controls on the occurrence and prevalence of floodplain channels in meandering rivers. Earth Surface Processes and Landforms **42**: 460–472.

Davidson SK, Hartley AJ, Weissmann GS, Nichols GJ, Scuderi LA. 2013. Geomorphic elements on modern distributive fluvial systems. Geomorphology **180-181**: 82-95.

Davidson SK, Leleu S, North CP (eds). 2011. From River to Rock Record: The Preservation of Fluvial Sediments and Their Subsequent Interpretation. SEPM, Special Publication **97**.

Dewey JF, Bird JM. 1970. Mountain belts and the new global tectonics. Journal of Geophysical Research **75**: 2625–2647.

Donselaar ME, Cuevas Gozalo MC, Moyano S. 2013. Avulsion processes at the terminus of low-gradient semi-arid fluvial systems: lessons from the Río Colorado, Altiplano endorheic basin, Bolivia. Sedimentary Geology **283**: 1–14.

Elger K, Oncken O, Glodny J. 2005. Plateau-style accumulation of deformation: Southern Altiplano. Tectonics **24**, TC4020.

Fagan SD, Nanson GC. 2004. The morphology and formation of floodplain-surface channels, Cooper Creek, Australia. Geomorphology **60**: 107–126.

Fisher JA, Krapf CBE, Lang SC, Nichols GJ, Payenberg THD. 2008. Sedimentology and architecture of the Douglas Creek terminal splay, Lake Eyre, central Australia. Sedimentology **55**: 1915–1930.

Gibling MR, Davies NS. 2012. Palaeozoic landscapes shaped by plant evolution. Nature Geoscience **5**: 99-105.

Grosjean M. 1994. Paleohydrology of the Laguna Lejía (north Chilean Altiplano) and climactic implications for late-glacial times. Palaeogeography, Palaeoclimatology, Palaeocology **109**: 89–100.

Hartley AJ, Weissmann GS, Nichols GJ, Warwick GL. 2010. Large distributive fluvial systems: characteristics, distribution, and controls on development. Journal of Sedimentary Research **80**: 167–183.

Horton BK, DeCelles PG. 2001. Modern and ancient fluvial megafans in the foreland basin system of the central Andes, southern Bolivia: implications for drainage network evolution in fold-thrust belts. Basin Research **13**: 43–63.

Horton BK, Hampton BA, Waanders GL. 2001. Paleogene synorogenic sedimentation in the Altiplano plateau and implications for initial mountain building in the central Andes. Geological Society of America Bulletin **113**: 1387–1400.

Ielpi A, Fralick P, Ventra D, Ghinassi M, Lebeau L, Marconato A, Meek R, Rainbird RH. 2018. Fluvial floodplains prior to greening of the continents: stratigraphic record, geodynamic setting, and modern analogues. Sedimentary Geology **372**: 140–172.

Isacks BL. 1988. Uplift of the central Andean plateau and bending of the Bolivian orocline. Journal of Geophysical Research **93**: 3211–3231.

Jordan TE, Reynolds JH, Erikson JP. 1997. Variability in age of initial shortening and uplift in the central Andes, 16-33.30'S. In Tectonic uplift and climate change, Ruddiman WF (ed). New York, Plenum Press: 41–61.

Kelly SB, Olsen H. 1993. Terminal fans — a review with reference to Devonian examples. In Current Research in Fluvial Sedimentology, Fielding CR (ed). Sedimentary Geology **85**: 339–374.

Lang SC, Payenberg THD, Reilly MRW, Hicks T, Benson JM, Kassan J. 2004. Modern analogues for dryland sandy fluvial–lacustrine deltas and terminal splay reservoirs. Australian Petroleum Production and Exploration Association Journal **44**: 329-355.

Larkin ZT, Ralph TJ, Tooth S, McCarthy TS. 2017. The interplay between extrinsic and intrinsic controls in determining floodplain wetland characteristics in the South African drylands. Earth Surface Processes and Landforms **42**: 1092–1109.

Lenters JD, Cook KH. 1999. Summertime precipitation variability over South America: role of the large-scale circulation. Monthly Weather Review **127**: 409–431.

Li J. 2014. Terminal fluvial systems in a semi-arid endorheic basin, Salar de Uyuni (Bolivia). Uitgeverij BOX Press: 's-Hertogenbosch, The Netherlands

Li J. 2018. Sedimentary model of fine-grained meandering river terminus systems in a semi-arid or arid endorheic basin. Earth Science, doi: 10.3799/dqkx.2018.525.

Li J, Bristow CS. 2015. Crevasse splay morphodynamics in a dryland river terminus: Río Colorado in Salar de Uyuni Bolivia. Quaternary International **377**: 71–82.

Li J, Bristow CS, Luthi SM, Donselaar ME. 2015a. Dryland anabranching river morphodynamics: Río Capilla, Salar de Uyuni, Bolivia. Geomorphology **250**: 282–297.

Li J, Donselaar ME, Hosseini Aria SE, Koenders R, Oyen AM. 2014a. Landsat imagery-based visualization of the geomorphological development at the terminus of a dryland river system. Quaternary International **352**: 100–110.

Li J, Menenti M, Mousivand A, Luthi SM. 2014b. Non-vegetated playa morphodynamics using multi-temporal Landsat imagery in a semi-arid endorheic basin: Salar de Uyuni, Bolivia. Remote Sensing **6**: 10131–10151.

Li J, Luthi SM, Donselaar ME, Weltje GJ, Prins MA, Bloemsma MR. 2015b. An ephemeral meandering river system: sediment dispersal processes in the Río Colorado, Southern Altiplano Plateau, Bolivia. Zeitschrift für Geomorphologie **59**: 301–317.

Li J, Yang X, Maffei C, Tooth S, Yao G. 2018. Applying independent component analysis on Sentinel-2 imagery to characterize geomorphological responses to an extreme flood event near the non-vegetated Río Colorado terminus, Salar de Uyuni, Bolivia. Remote Sensing **10**: 725 (19 pp.).

Marshall LG, Swisher CC III, Lavenu A, Hoffstetter R, Curtis GH. 1992. Geochronology of the mammal-bearing late Cenozoic on the northern Altiplano, Bolivia. Journal of South American Earth Sciences **5**: 1–19.

Mertes LA, Dunne T, Martinelli LA. 1996. Channel–floodplain geomorphology along the Solimões-Amazon river, Brazil. Geological Society of America Bulletin **108**: 1089–1107.

Miall AD. 1996. The Geology of Fluvial Deposits: Sedimentary Facies, Basin Analysis, and Petroleum Geology. Springer, Berlin.

Milan DM, Heritage G, Tooth S, Entwistle N. 2018. Morphodynamics of bedrock-influenced dryland rivers during extreme floods: insights from the Kruger National Park, South Africa. Geological Society of America Bulletin **130**: in press.

Millard C, Hajek E, Edmonds DA. 2017. Evaluating controls on crevasse-splay size: implications for floodplain-basin filling. Journal of Sedimentary Research **87**: 722-739.

Mjøs R, Walderhaug O, Prestholm E. 1993. Crevasse splay sandstone geometries in the Middle Jurassic Ravenscar Group of Yorkshire, UK. In Alluvial Sedimentation, Marzo M, Puigdefábregas C. (eds). International Association of Sedimentologists, Special Publication **17**: 167–184.

Mukerji AB. 1976. Terminal fans of inland streams in Sutlej–Yamuna Plain, India. Zeitschrift für Geomorphologie **20**: 190–204.

Pickup G. 1985. The erosion cell — a geomorphic approach to landscape classification in range assessment. Australian Rangeland Journal **7**: 114–121.

Pickup G. 1991. Event frequency and landscape stability on the floodplain systems of arid central Australia. Quaternary Science Reviews **10**: 463–473.

Placzek CJ, Quade J, Patchett PJ. 2013. A 130 ka reconstruction of rainfall on the Bolivian Altiplano. Earth and Planetary Science Letters **363**: 97–108.

Rigsby CA, Bradbury JP, Baker PA, Rollins SM, Warren MR. 2005. Late Quaternary palaeolakes, rivers, and wetlands on the Bolivian Altiplano and their palaeoclimatic implications. Journal of Quaternary Science **20**: 671–691.

Risacher F, Fritz B. 2009. Origin of salts and brine evolution of Bolivian and Chilean salars. Aquatic Geochemistry **15**: 123–157.

Sandén AB. 2016. Process-based modelling of a crevasse splay (MSc. thesis). Technische Universiteit Delft, Delft, The Netherlands.

Stølum HH. 1998. Planform geometry and dynamics of meandering rivers. Geological Society of America Bulletin **110**: 1485–1498.

Tooth S. 1999a. Floodouts in central Australia. In Varieties of Fluvial Form, Miller AJ, Gupta A. (eds). Chichester: John Wiley and Sons: 219-247.

Tooth S. 1999b. Downstream changes in floodplain character on the Northern Plains of arid central Australia. In Fluvial Sedimentology VI, Smith ND, Rogers J. (eds). International Association of Sedimentologists, Special Publication **28**: 99–112. Blackwell Scientific Publications, Oxford.

Tooth S. 2000a. Process, form and change in dryland rivers: a review of recent research. Earth-Science Reviews **51**: 67-107.

Tooth S. 2000b. Downstream changes in dryland river channels: the Northern Plains of arid central Australia. Geomorphology **34**: 33-54.

Tooth S. 2004. ‘Floodout’. In Encyclopedia of Geomorphology, Goudie AS. (ed). London: Routledge, Volume **1**: 380-381.

Tooth S. 2005. Splay formation along the lower reaches of ephemeral rivers on the Northern Plains of arid central Australia. Journal of Sedimentary Research **75**: 634-647.

Tooth S. 2013, Dryland fluvial environments: assessing distinctiveness and diversity from a global perspective.  In Treatise on Geomorphology, Shroder J, Wohl EE. (eds). Fluvial Geomorphology **9**, Academic Press, San Diego, CA: 612-644.

Tooth S, McCarthy TS, Hancox PJ, Brandt D, Buckley K, Nortje E, McQuade S. 2002. The geomorphology of the Nyl River and floodplain in the semi-arid Northern Province, South Africa. South African Geographical Journal **84**: 226-237.

Tooth S, Hancox PJ, Brandt D, McCarthy TS, Jacobs Z, Woodborne SM. 2013. Controls on the genesis, sedimentary architecture, and preservation potential of dryland alluvial successions in stable continental interiors: insights from the incising Modder River, South Africa. Journal of Sedimentary Research **83**: 541-561.

Tooth S, McCarthy T, Rodnight H, Keen-Zebert A, Rowberry M, Brandt D. 2014. Late Holocene development of a major fluvial discontinuity in floodplain wetlands of the Blood River, eastern South Africa. Geomorphology **205**: 128–141.

Torres Carranza YA. 2013. Static Reservoir Model of Crevasse Splays in the Colorado River system, Salar de Uyuni, Bolivia (MSc. thesis). Technische Universiteit Delft, Delft, The Netherlands.

Trigg MA, Bates PD, Wilson MD, Schumann G, Baugh C. 2012. Flood-plain channel morphology and networks of the middle Amazon River. Water Resources Research **48**. DOI:10.1029/2012WR011888.

United Nations Environment Program (UNEP), 1992. World Atlas of Desertification. Edward Arnold, London: 15–45.

van den Berg JH. 1995. Prediction of alluvial channel pattern of perennial rivers. Geomorphology **12**: 259–279.

van Toorenenburg KA, Donselaar ME, Noordijk NA, Weltje GJ. 2016. On the origin of crevasse-splay amalgamation in the Huesca fluvial fan (Ebro Basin, Spain): implications for connectivity in low net-to-gross fluvial deposits. Sedimentary Geology **343**: 156-164.

Wakelin-King GA, Webb JA. 2007. Threshold-dominated fluvial styles in an arid-zone mud-aggregate river: the uplands of Fowlers Creek, Australia. Geomorphology **85**: 114–127.

Weissmann GS, Hartley AJ, Nichols GJ, Scuderi LA, Olson M, Buehler H, Banteah R. 2010. Fluvial form in modern continental sedimentary basins: distributive fluvial systems. Geology **38:** 39–42 (includes data repository item 2010006).

## Figure captions

Fig. 1. Characteristics of the Altiplano and the lower Río Colorado: A) location of the Altiplano in South America; B) map of the Altiplano; C) the lower reaches of the Río Colorado approaching the southeastern margin of Salar de Uyuni, with boxes indicating the areas covered by subsequent figures; and D) field photograph showing the non-vegetated nature of the study area and an abandoned floodplain channel (view looking upstream along the abandoned channel. For location, see Fig. 7D). Parts A and B are modified after Placzek et al. (2013).

Fig. 2 Annual precipitation total and maximum daily precipitation for the period 1976-2017 (Source: Bolivian Servicio Nacional de Meteorología e Hidrología). Vertical blue lines with arrows indicate the dates of satellite imagery used in this study (Table 1).

Fig. 3. Example of the development of a chute cutoff between 2004 and 2016 (for location, see Fig. 1C). On the adjacent floodplain, erosion cells have developed, with letters S, T and F representing the scour, transport and fill sections. A is QuickBird-2 imagery; B is WorldView-2 imagery; C and D are Pléiades imagery. In all images, general flow direction is from bottom to top, and north is oriented to the top.

Fig. 4. Example of significant erosion of a floodplain channel that was accompanied by chute cutoff development and filling, as well as crevasse splay development between 2004 and 2016 (for location, see Fig. 1C and for details, see Fig. 5). A is QuickBird-2 imagery; B is WorldView-2 imagery; C and D are Pléiades imagery. In all images, general flow direction is from right to left, and north is oriented to the top.

Fig. 5. Details of the floodplain channel shown in Figure 4. Different colour arrows indicate the development of various new crevasse splays (NCS1, NCS2, NCS3). A is QuickBird-2 imagery; B is WorldView-2 imagery; C and D are Pléiades imagery. In all images, general flow direction is from right to left, and north is oriented to the top.

Fig. 6. Examples of the morphodynamics of channels and crevasse splays near the terminus (floodout) of a floodplain channel between 2004 and 2016 (for location, see Fig. 1C). A is QuickBird-2 imagery; B is WorldView-2 imagery; C and D are Pléiades imagery. In all images, general flow direction is from lower right to upper left, and north is oriented to the top.

Fig. 7. Examples of the development of erosion cells along an abandoned channel from 2004 to 2016 (for location, see Fig. 1C). Development of erosion cells EC1 through EC4 was associated with the location of remnant crevasse splays CS1 through CS4. Letters S, T and F represent scour, transport and fill sections in the erosion cells. The red dot at D indicates the location of the photograph in Fig. 1D. A is QuickBird-2 imagery; B is WorldView-2 imagery; C and D are Pléiades imagery. In all images,

general flow direction is from lower right to upper left (i.e. oblique to the abandoned channels – see Fig. 8), and north is oriented to the top.

Fig. 8. Orientations of the flow directions of currently active crevasse splays that diverge from the trunk Río Colorado (flow direction from lower right to left) compared to the orientation of erosion cells along an abandoned channel (for location, see Fig. 1C). All bearings are in degrees. The dashed line indicates the measurement path of high precision GPS and the red dot (see equivalent in Fig. 11A) indicates the downstream end of the profile. The image is Pléiades imagery.

Fig. 9. Example of the interaction between crevasse splays at a channel terminus (floodout) and downstream erosion cells (for location, see Fig. 1C, and for details of the crevasse splays, see Fig. 6). In B, letters S, T and F represent scour, transport and fill sections in the erosion cells. A is Pléiades imagery, with general flow direction from lower right to upper left, and north oriented to the top.

Fig. 10. Satellite image-based comparison of the geometry and hydraulics of the trunk channel of the Río Colorado in 2004 and 2013, as measured downstream from the bridge across the river (Fig. 1C, see red dot in lower right): A) downstream variations in channel width, showing an exponential width decrease between 0 and 17 km downstream, and a more linear decrease thereafter; b) comparison of channel width in 2004 and 2013, showing a slight overall increase in width; C) comparison of estimated bankfull discharge in 2004 and 2013, showing a slight overall increase in discharge; D) comparison of specific stream power in 2004 and 2013, showing a slight overall increase in stream power.

Fig. 11. Results of high-precision GPS measurements: A) high-precision GPS elevation profile along a crevasse splay (see the dashed line in Fig. 8) with the red dot indicating the downstream end of the profile; B) GPS-derived contour map (0.1 m interval) covering the location of an erosion cell and floodout (for location, see Fig. 1C). The black lines are GPS measurement paths; C) reconstruction of the surface topography of the erosion cell in B using resampling method of nearest neighbours, with letters S, T and F representing the scour, transport and fill sections.

Fig. 12. Examples showing the linear distribution and alignment of erosion cells between abandoned channels (for location, see Fig. 1C). Letters S, T and F represent the scour, transport and fill sections in the erosion cells. All images are Pléiades imagery, with general flow direction from bottom to top, and north oriented to the top.

Fig. 13. Example of a relatively straight channel that may have resulted from the elongation and connection of erosion cells (for location, see Fig. 1C). The straightness of this channel contrasts with the higher sinuosity evident along older active or

abandoned channels. The image is Pléiades imagery, with general flow direction from bottom to top, and north oriented to the top.

Fig. 14. Examples of erosion cells in the lower reaches of other dryland rivers: A) the Amargosa River in Death Valley, California, USA. The image is from Google Earth™, with general flow direction from bottom to top, and north oriented to the top; B) on the margins of salt lakes near the Huobusun Lake in northwestern China. The image is from Google Earth™, with general flow direction from lower right to upper left, and north oriented to the top.

# Tables

Table1 Information regarding the high resolution satellite imagery used in this study

| Type | Catalog ID | Acq. date | Avg. off nadir angle | Avg. target azimuth | Sensor |
|---|---|---|---|---|---|
| QuickBird-2 (Google Earth) | 10100100035DE200 | Nov 2, 2004 | 8° | 293° | QB-2 |
| | 1010010004912500 | Oct 5, 2005 | 8° | 261° | QB-2 |
| WorldView-2 | 1020010001455700 | Dec 30, 2007 | 17° | 85° | WV-1 |
| | 10300100083DC100 | Jan 3, 2011 | 26° | 221° | WV-2 |
| Pléiades | DS_PHR1B_201307131443591_SE1_PX_W067S21_0310_02391 | Jul 13, 2013 | 16° | 33° | PHR1B |
| | DS_PHR1B_201307201441038_SE1_PX_W067S21_0115_05305 | Jul 20, 2013 | 18° | 36° | PHR1B |
| | DS_PHR1B_201603011443021_FR1_PX_W067S21_0310_02408 | Mar 01, 2016 | 11° | 69° | PHR1B |

Table 2 Characteristics of floodplain channels near the Río Colorado river terminus.  EC is erosion cell.

| Locality | Floodplain gradient (m $m^{-1}$) | Width (m) | Depth (m) | Cross-sectional area ($m^2$) | Bankfull discharge ($m^3$ $s^{-1}$) | Specific stream power (W $m^{-2}$) |
|---|---|---|---|---|---|---|
| Chute cutoff (Fig. 3) | 0.00037 | 15.84 | 1.43 | 22.64 | 22.27 | 5 |
| Eroded channel (Fig. 4) | 0.00023 | 24.82 | 1.69 | 41.84 | 46.52 | 4.25 |
| Floodout - EC (Fig. 6) | 0.00022 | 13.1 | 0.571 | 7.48 | 16.31 | 2.78 |
| Crevasse splay (Fig. 8) | 0.00059 | 8 | 0.3 | 2.4 | 7.27 | 5.36 |

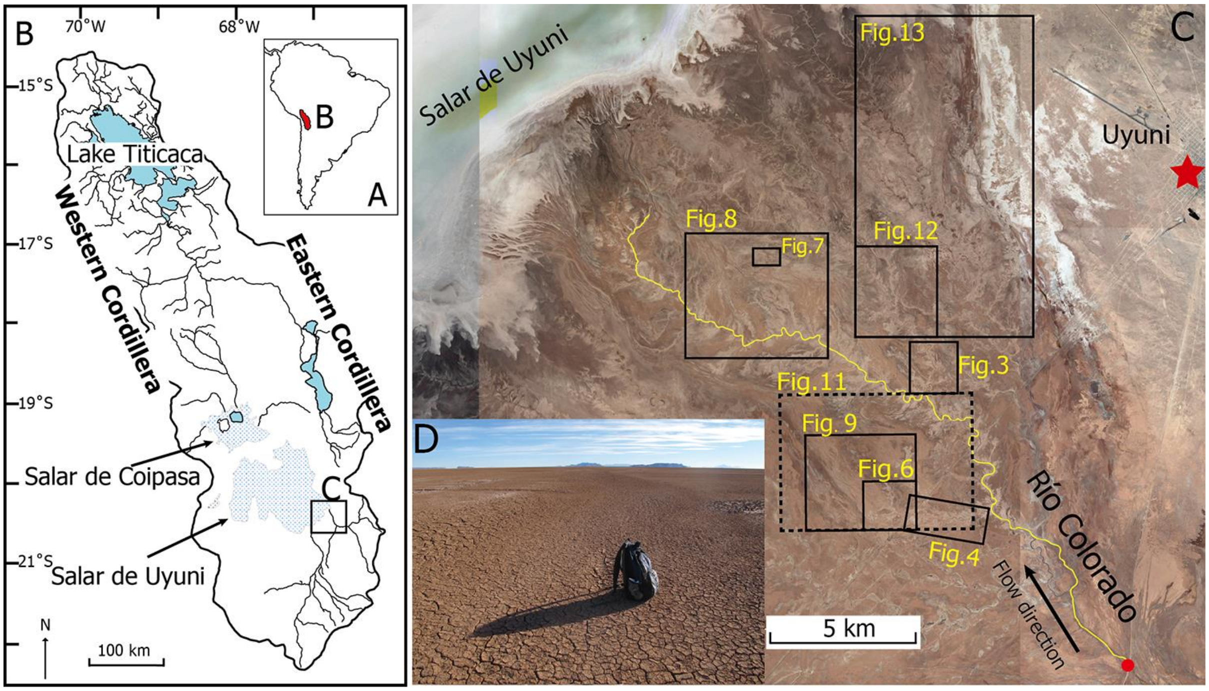
B
70°W
68°W
15°S
17°S
19°S
21°S
Lake Titicaca
Western Cordillera
Eastern Cordillera
Salar de Coipasa
Salar de Uyuni
C
A
B
N
100 km
Salar de Uyuni
Fig.13
Uyuni
Fig.12
Fig.8
Fig.7
Fig.3
Fig.11
Fig. 9
Fig.6
Fig.4
Río Colorado
Flow direction
5 km
D

Fig. 1

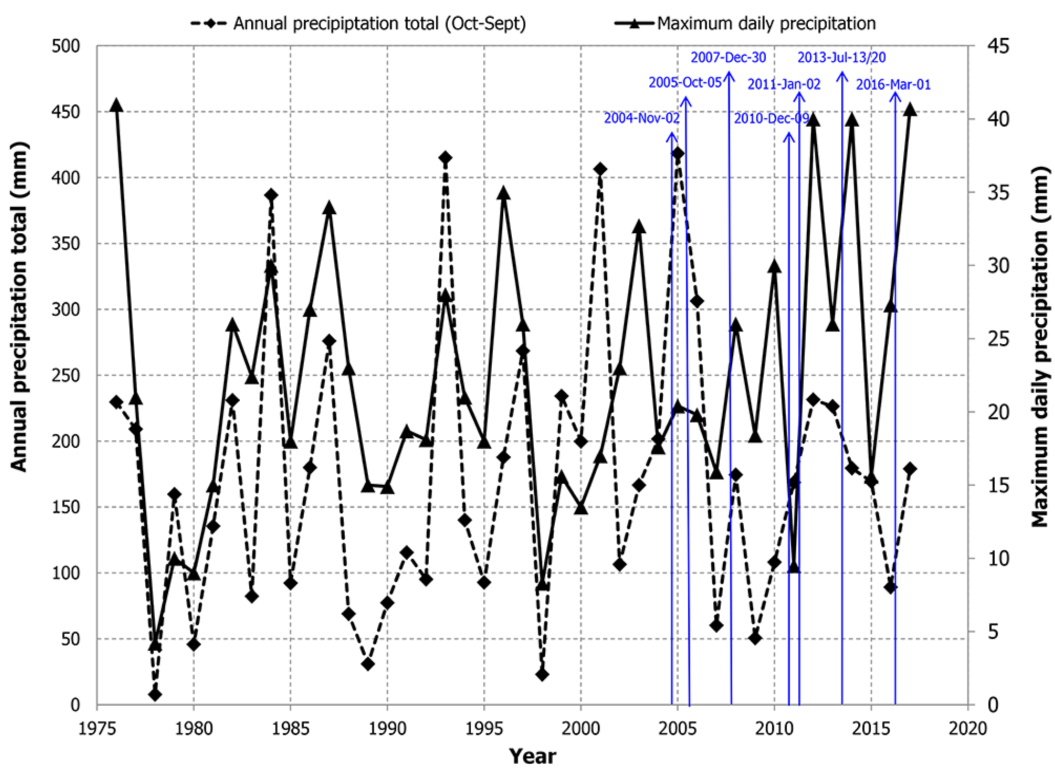
Annual precipiptation total (Oct-Sept)
Maximum daily precipitation
Annual precipitation total (mm)
Maximum daily precipitation (mm)
Year
2004-Nov-02
2005-Oct-05
2007-Dec-30
2010-Dec-09
2011-Jan-02
2013-Jul-13/20
2016-Mar-01
0
50
100
150
200
250
300
350
400
450
500
0
5
10
15
20
25
30
35
40
45
1975
1980
1985
1990
1995
2000
2005
2010
2015
2020

Fig. 2

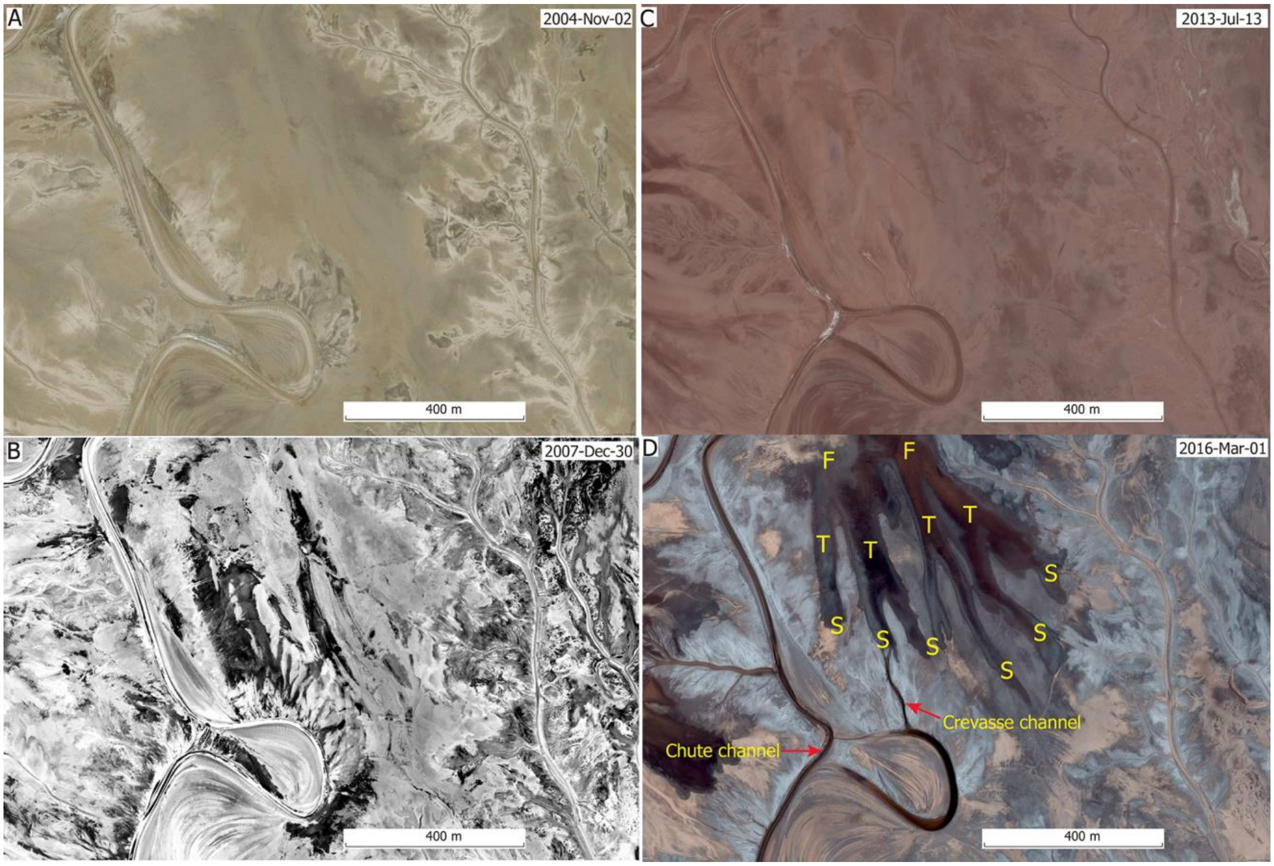
A
2004-Nov-02
400 m
C
2013-Jul-13
400 m
B
2007-Dec-30
400 m
D
2016-Mar-01
F
F
T
T
T
T
S
S
S
S
S
S
Crevasse channel
Chute channel
400 m

Fig. 3

957

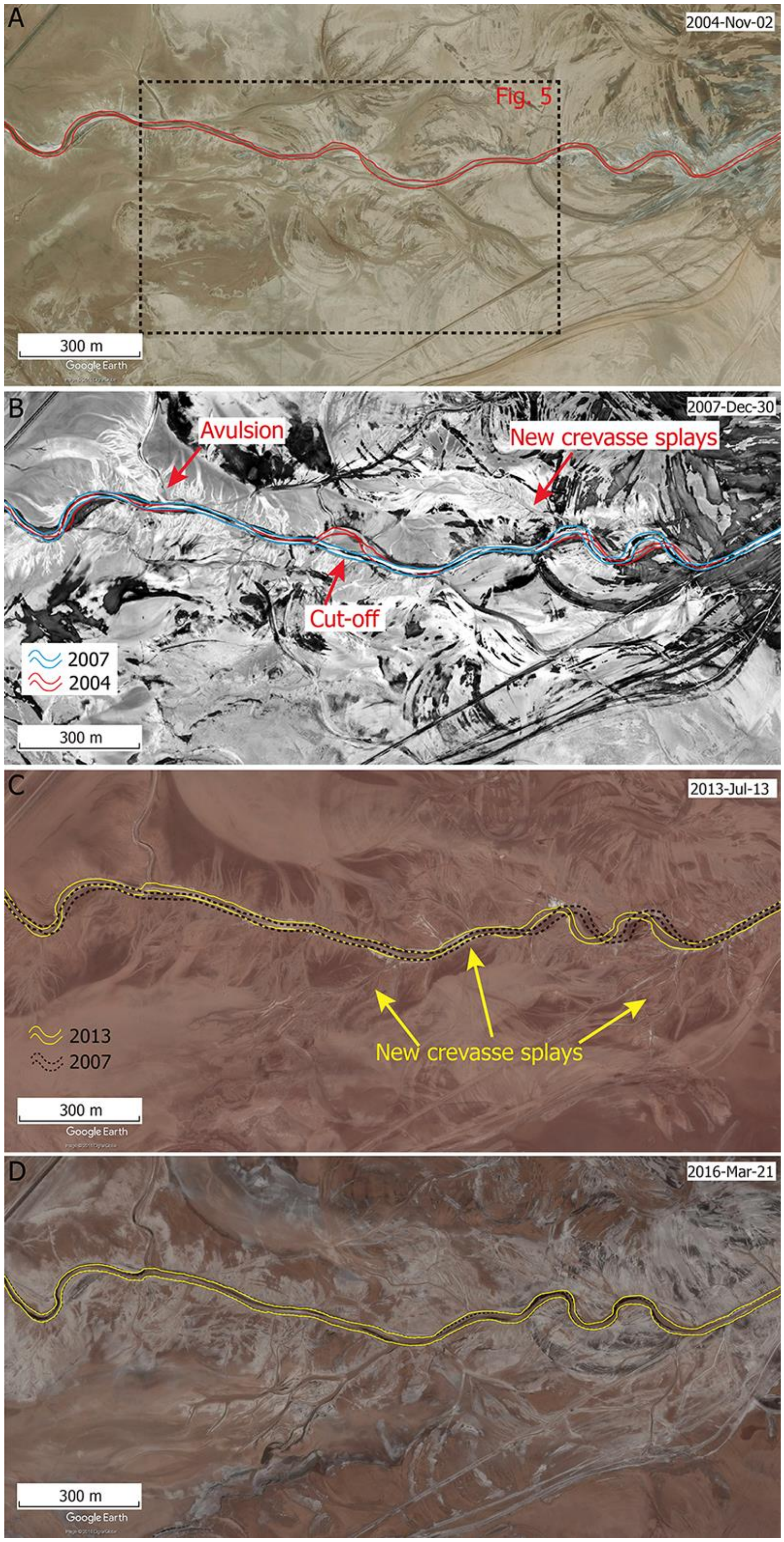
A
2004-Nov-02
Fig. 5
300 m
Google Earth
B
2007-Dec-30
Avulsion
New crevasse splays
Cut-off
2007
2004
300 m
C
2013-Jul-13
2013
2007
New crevasse splays
300 m
Google Earth
D
2016-Mar-21
300 m
Google Earth

958 Fig. 4

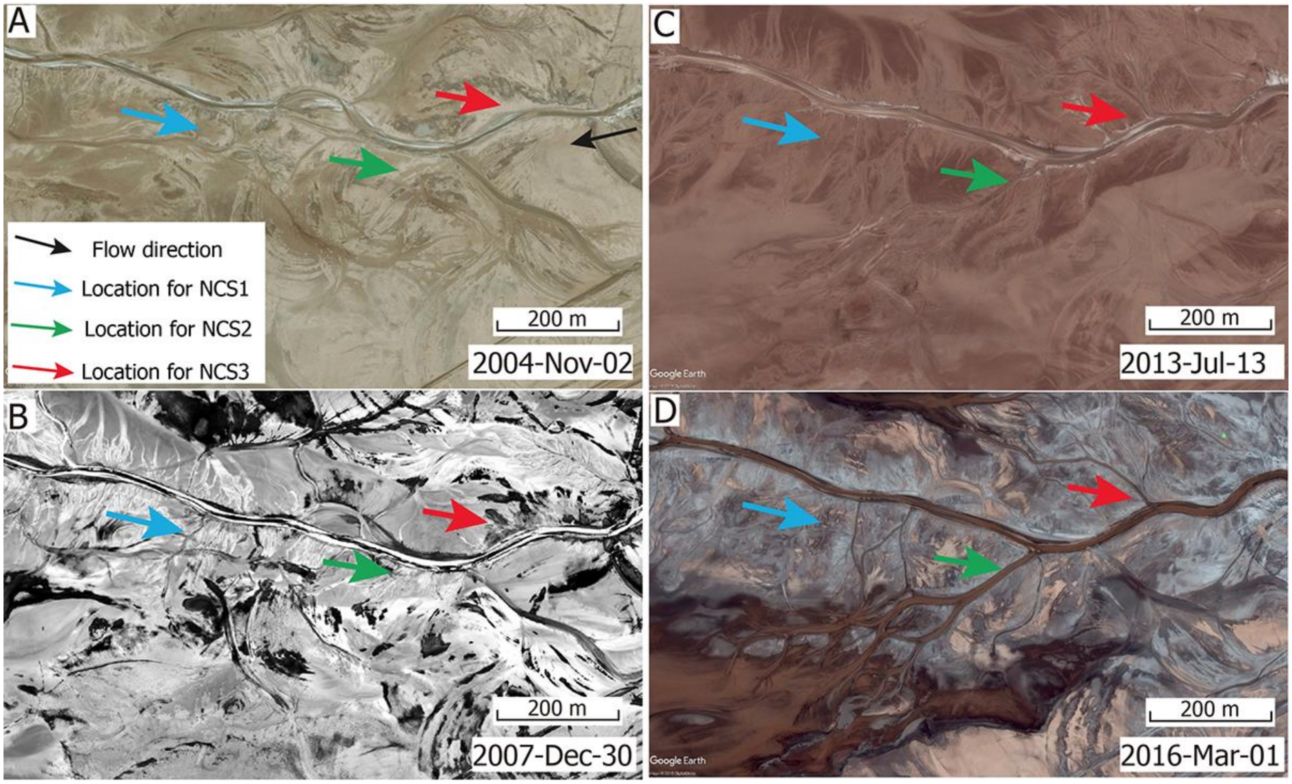
A
Flow direction
Location for NCS1
Location for NCS2
Location for NCS3
200 m
2004-Nov-02
B
200 m
2007-Dec-30
C
Google Earth
200 m
2013-Jul-13
D
Google Earth
200 m
2016-Mar-01

Fig. 5

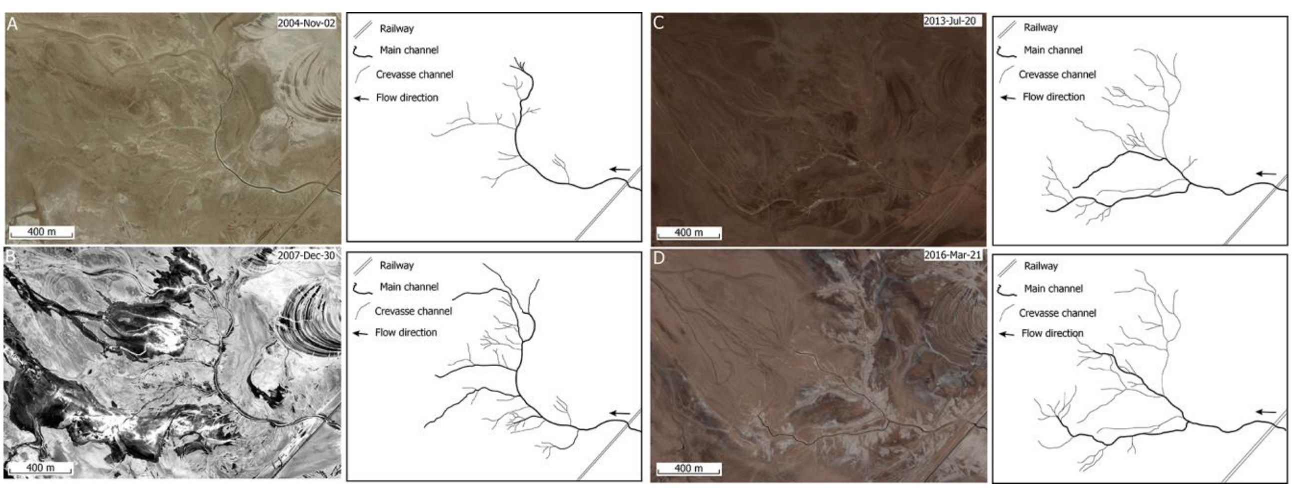
A
2004-Nov-02
400 m
Railway
Main channel
Crevasse channel
Flow direction
B
2007-Dec-30
400 m
Railway
Main channel
Crevasse channel
Flow direction
C
2013-Jul-20
400 m
Railway
Main channel
Crevasse channel
Flow direction
D
2016-Mar-21
400 m
Railway
Main channel
Crevasse channel
Flow direction

Fig. 6

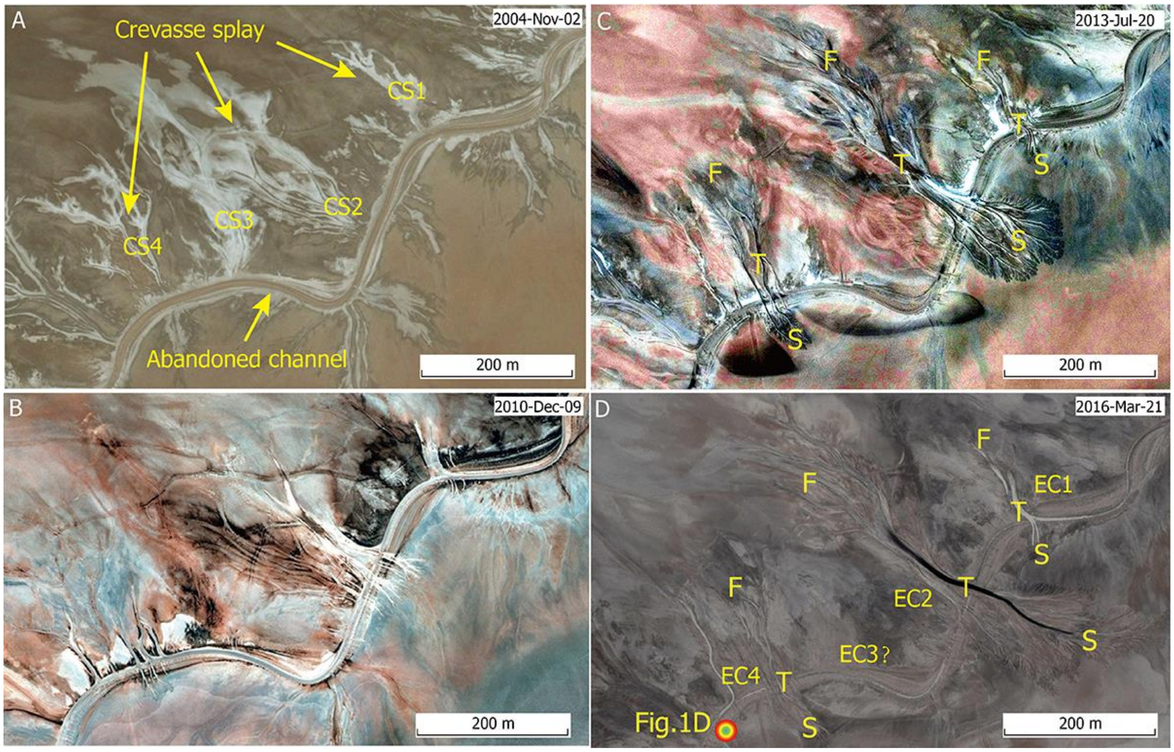
A
2004-Nov-02
Crevasse splay
CS1
CS2
CS3
CS4
Abandoned channel
200 m
B
2010-Dec-09
200 m
C
2013-Jul-20
F
T
S
200 m
D
2016-Mar-21
F
T
S
EC1
EC2
EC3?
EC4
Fig.1D
200 m

Fig. 7

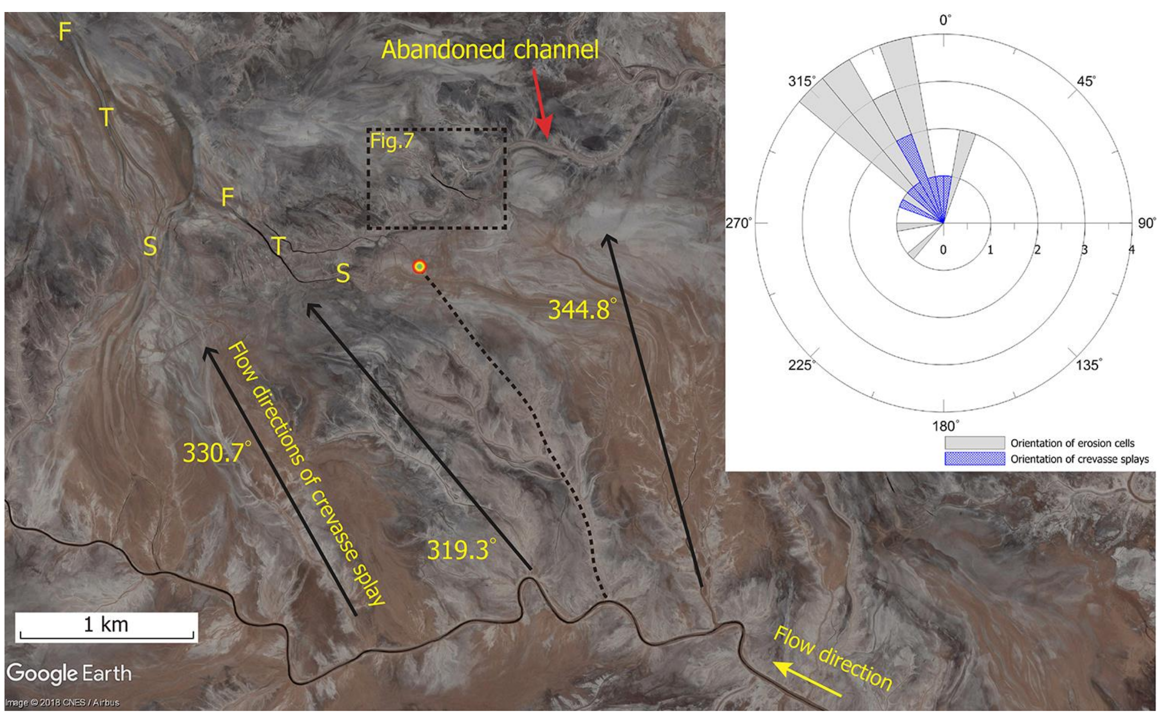
F
T
S
Abandoned channel
Fig.7
344.8°
330.7°
319.3°
Flow directions of crevasse splay
Flow direction
1 km
Google Earth
Image © 2018 CNES / Airbus
0°
45°
90°
135°
180°
225°
270°
315°
0
1
2
3
4
Orientation of erosion cells
Orientation of crevasse splays

Fig. 8

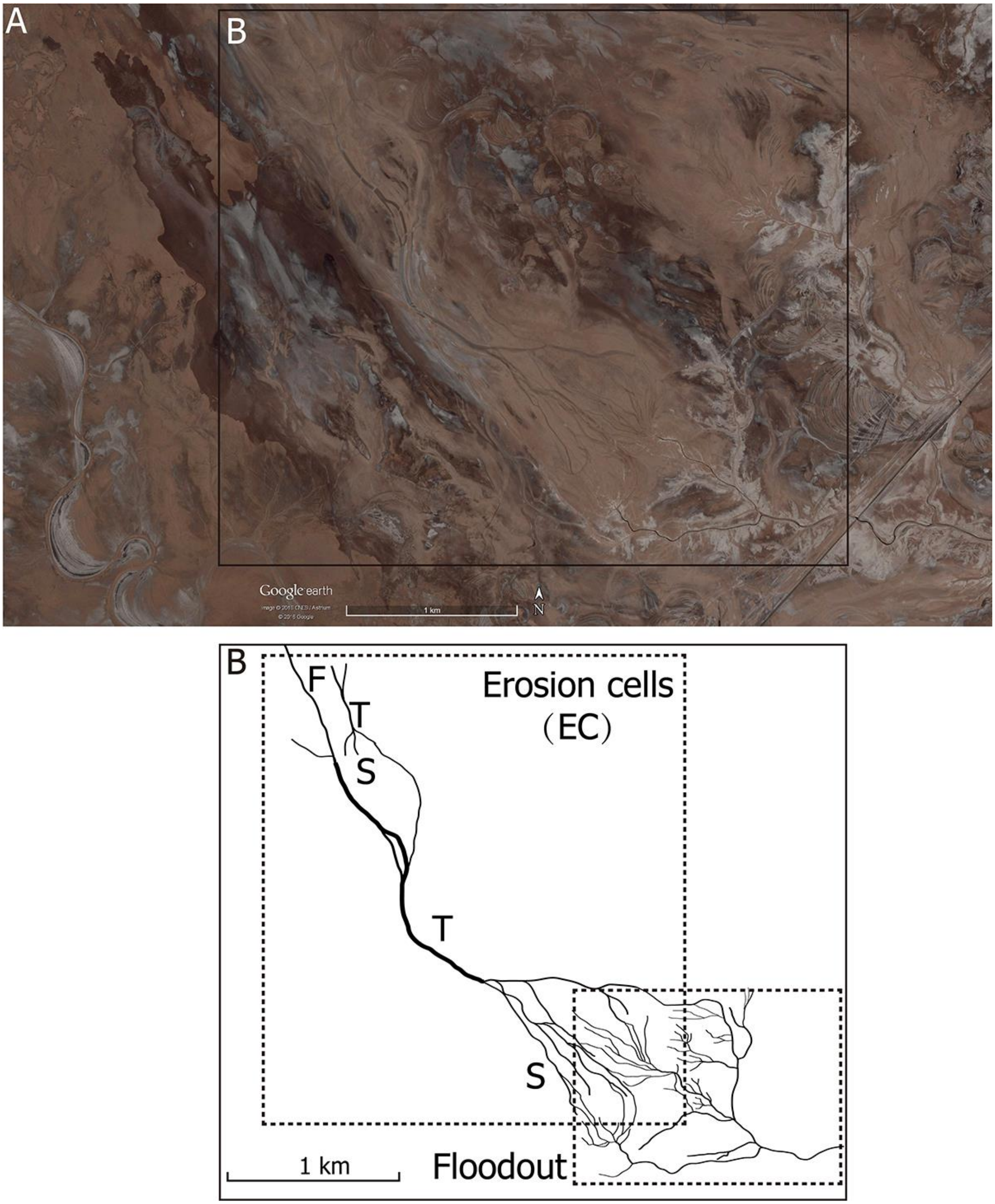


Fig. 9

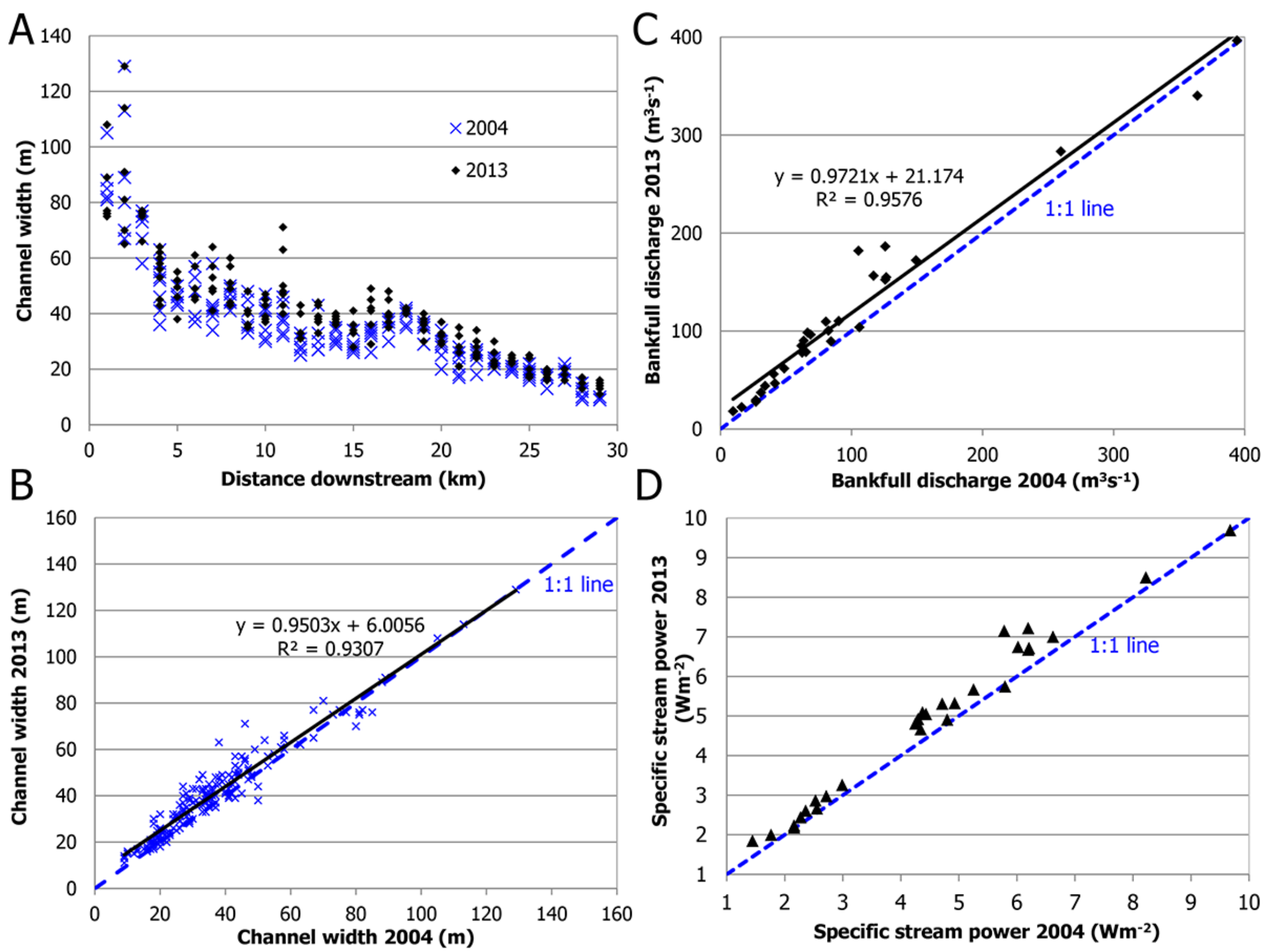

A
Channel width (m)
Distance downstream (km)
2004
2013
B
Channel width 2013 (m)
Channel width 2004 (m)
y = 0.9503x + 6.0056
R² = 0.9307
1:1 line
C
Bankfull discharge 2013 (m³s⁻¹)
Bankfull discharge 2004 (m³s⁻¹)
y = 0.9721x + 21.174
R² = 0.9576
1:1 line
D
Specific stream power 2013 (Wm⁻²)
Specific stream power 2004 (Wm⁻²)
1:1 line


Fig. 10

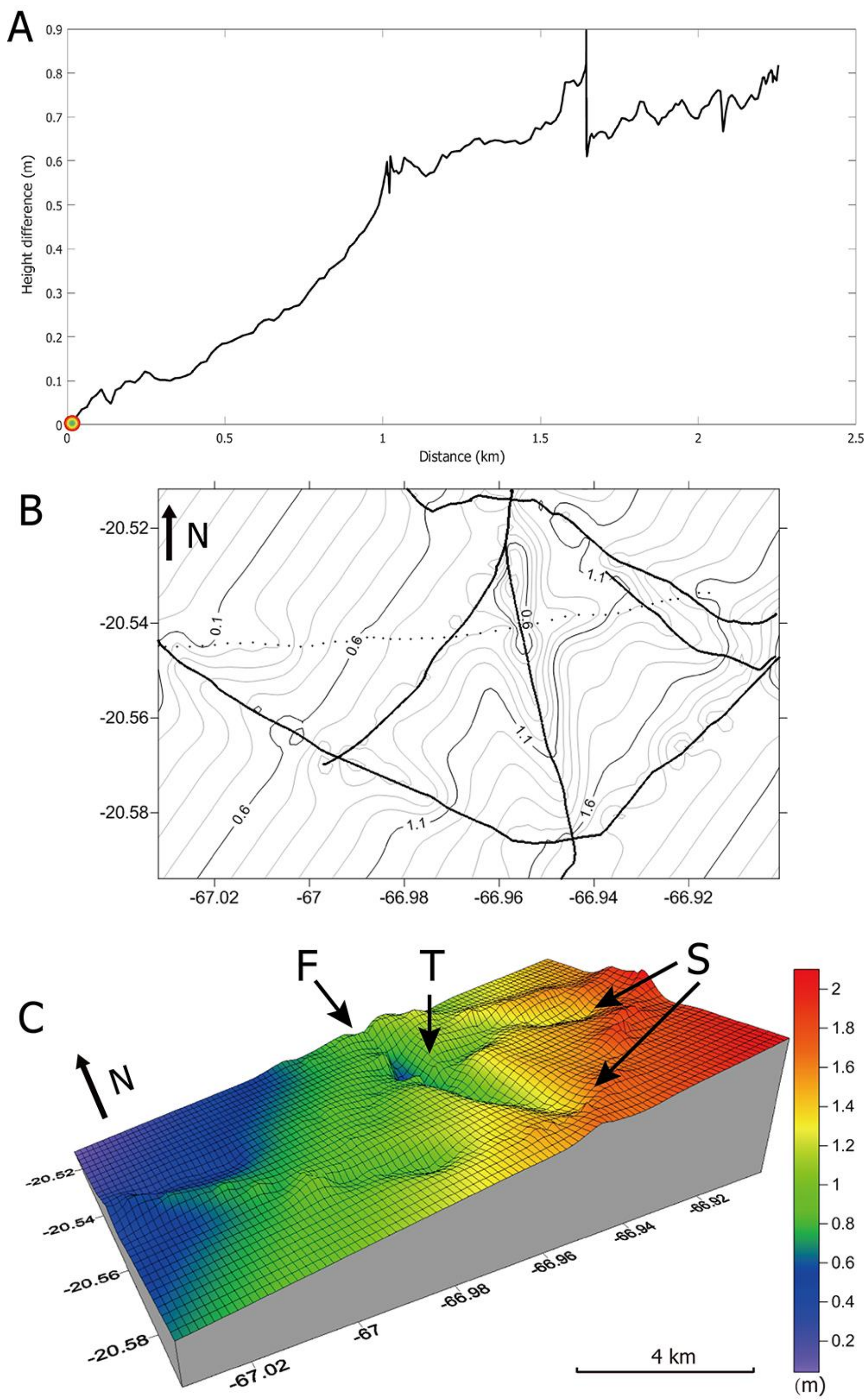
A
Height difference (m)
Distance (km)
0.9
0.8
0.7
0.6
0.5
0.4
0.3
0.2
0.1
0
0
0.5
1
1.5
2
2.5
B
N
-20.52
-20.54
-20.56
-20.58
-67.02
-67
-66.98
-66.96
-66.94
-66.92
0.1
0.6
0.6
1.1
1.1
1.1
1.6
0.6
C
F
T
S
N
-20.52
-20.54
-20.56
-20.58
-67.02
-67
-66.98
-66.96
-66.94
-66.92
4 km
2
1.8
1.6
1.4
1.2
1
0.8
0.6
0.4
0.2
(m)

Fig. 11

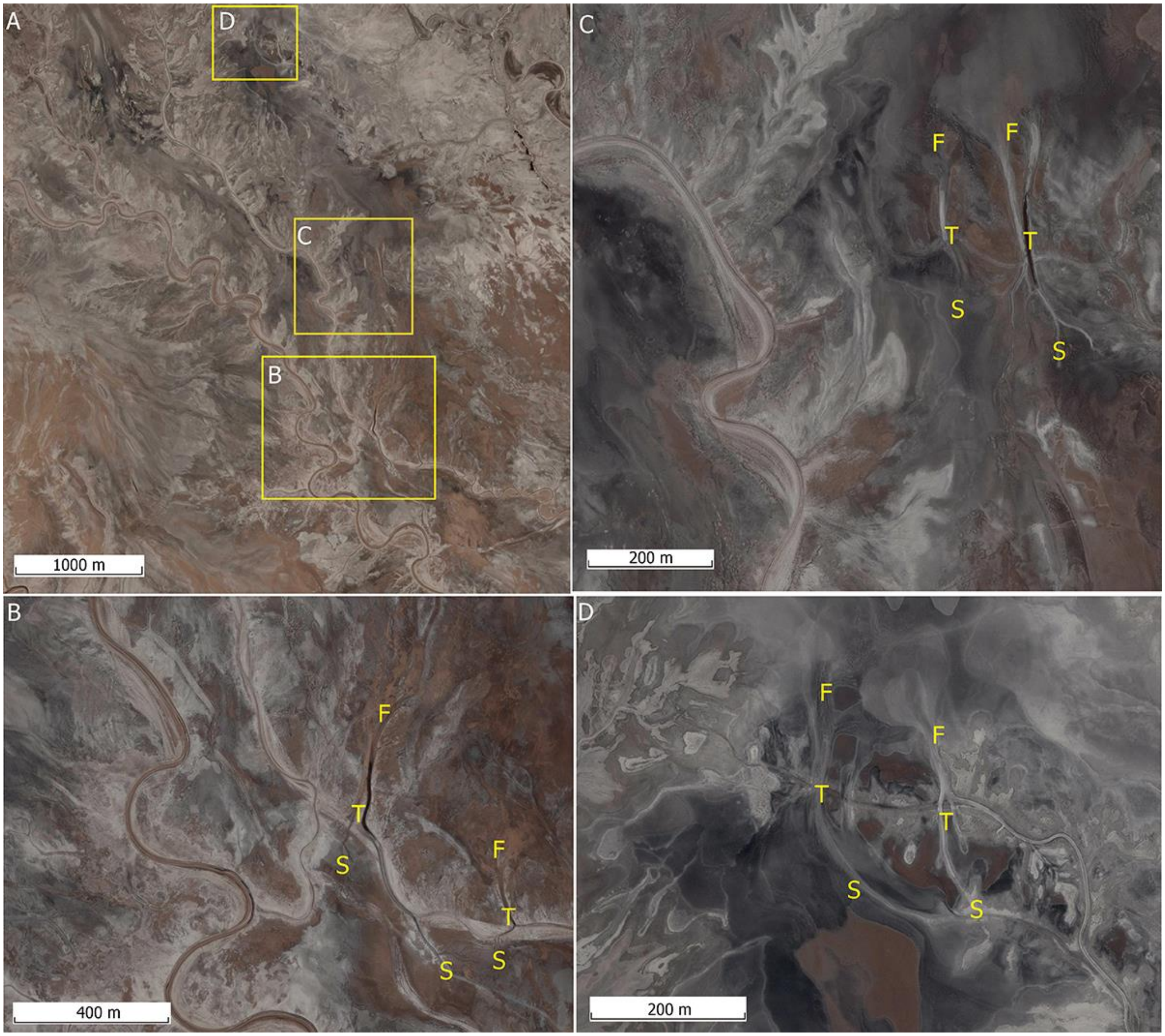


Fig. 12

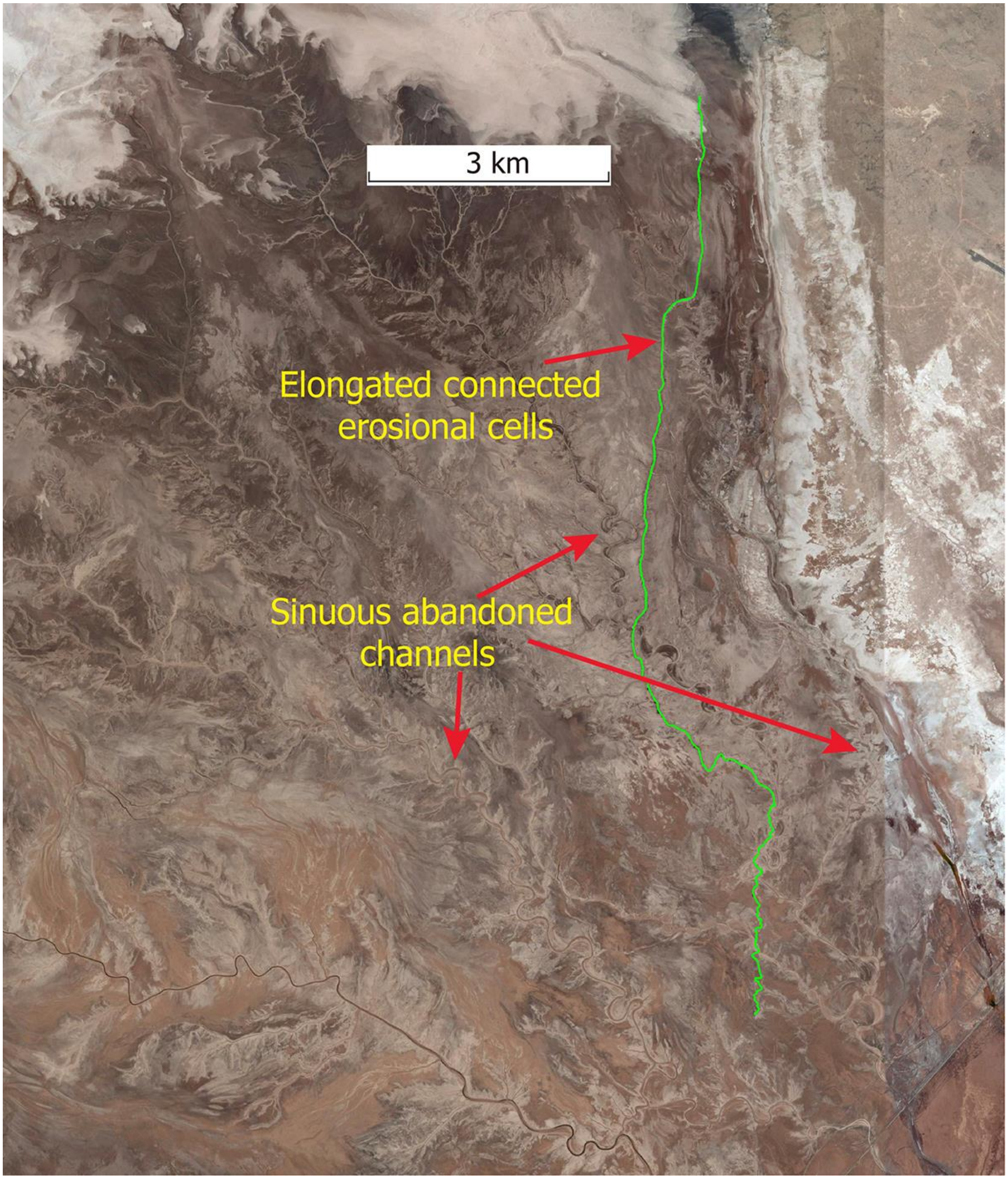
3 km
Elongated connected erosional cells
Sinuous abandoned channels

Fig. 13

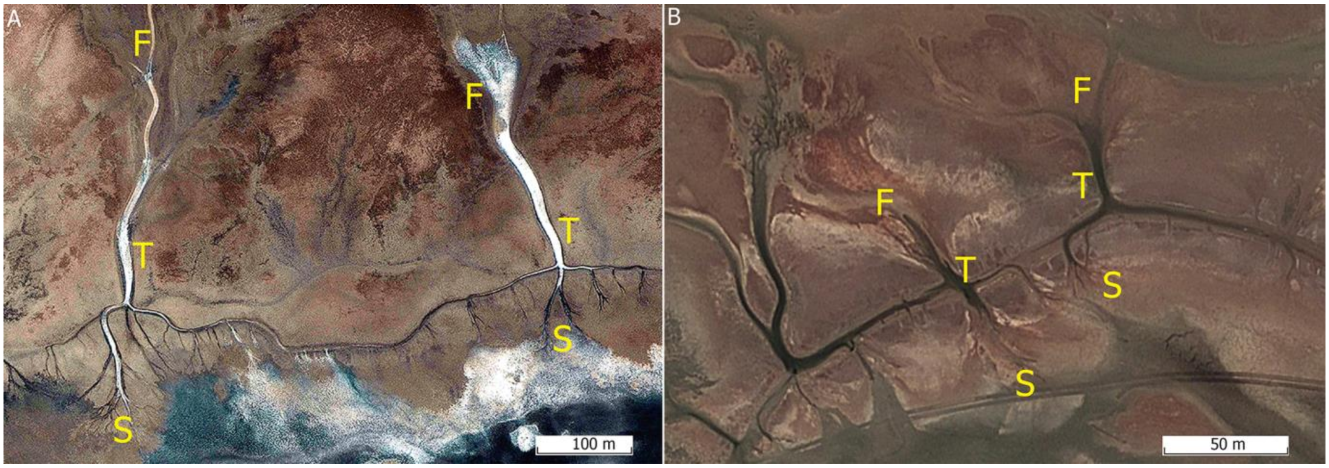


Fig. 14